

Review on flexible perovskite photodetector: processing and applications

Xuning ZHANG^a, Xingyue LIU^b, Yifan HUANG^a, Bo SUN^c, Zhiyong LIU^{a,d}, Guanglan LIAO (✉)^{a,d}, Tielin SHI (✉)^a

^a State Key Laboratory of Digital Manufacturing Equipment and Technology, Huazhong University of Science and Technology, Wuhan 430074, China

^b School of Mechanical Engineering and Electronic Information, China University of Geoscience (Wuhan), Wuhan 430074, China

^c School of Aerospace Engineering, Huazhong University of Science and Technology, Wuhan 430074, China

^d Shenzhen Huazhong University of Science and Technology Research Institute, Shenzhen 518100, China

✉ Corresponding author. E-mails: guanglan.liao@hust.edu.cn (Guanglan LIAO); tlshi@hust.edu.cn (Tielin SHI)

© The Author(s) 2023. This article is published with open access at link.springer.com and journal.hep.com.cn

ABSTRACT Next-generation optoelectronics should possess lightweight and flexible characteristics, thus conforming to various types of surfaces or human skins for portable and wearable applications. Flexible photodetectors as fundamental devices have been receiving increasing attention owing to their potential applications in artificial intelligence, aerospace industry, and wise information technology of 120, among which perovskite is a promising candidate as the light-harvesting material for its outstanding optical and electrical properties, remarkable mechanical flexibility, low-cost and low-temperature processing methods. To date, most of the reports have demonstrated the fabrication methods of the perovskite materials, materials engineering, applications in solar cells, light-emitting diodes, lasers, and photodetectors, strategies for device performance enhancement, few can be seen with a focus on the processing strategies of perovskite-based flexible photodetectors, which we will give a comprehensive summary, herein. To begin with, a brief introduction to the fabrication methods of perovskite (solution and vapor-based methods), device configurations (photovoltaic, photoconductor, and phototransistor), and performance parameters of the perovskite-based photodetectors are first arranged. Emphatically, processing strategies for photodetectors are presented following, including flexible substrates (i.e., polymer, carbon cloth, fiber, paper, etc.), soft electrodes (i.e., metal-based conductive networks, carbon-based conductive materials, and two-dimensional (2D) conductive materials, etc.), conformal encapsulation (single-layer and multilayer stacked encapsulation), low-dimensional perovskites (0D, 1D, and 2D nanostructures), and elaborate device structures. Typical applications of perovskite-based flexible photodetectors such as optical communication, image sensing, and health monitoring are further exhibited to learn the flexible photodetectors on a deeper level. Challenges and future research directions of perovskite-based flexible photodetectors are proposed in the end. The purpose of this review is not only to shed light on the basic design principle of flexible photodetectors, but also to serve as the roadmap for further developments of flexible photodetectors and exploring their applications in the fields of industrial manufacturing, human life, and health care.

KEYWORDS photodetector, perovskite, flexible, processing, application

1 Introduction

Technologies have witnessed rapid development over the past few decades, and the concepts of foldable, portable, and bendable have been mentioned more and more. Flexible optoelectronic devices have become an emerging field at the forefront of multidisciplinary research

worldwide [1]. The photodetector, detecting and measuring the characteristics of light (wavelength, intensity, polarization, etc.) through the photoelectric effect has been obtaining growing attention in the fields of research and industry. Under light illumination, semiconductor materials in the device absorb light photons and generate photocurrent through the effects of photovoltaic or photoconductive. Flexible photodetectors as the fundamental components of flexible optoelectronic systems

have been playing significant roles in modern industrial production, basic scientific research, medical diagnosis, military defense, and other fields [2–5]. For example, when attached to the human body, flexible photodetectors can detect people's physiological signals without affecting their daily activities. Thus, further research on flexible photodetectors is important for the time being.

In photodetectors, semiconductor materials are essential for absorbing incident light and generating electron-hole (e-h) pairs. The e-h pairs are then separated into electrons and holes under built-in or external electric fields and finally collected by the paired electrodes to generate an electric current. Through this process, conversion from the light signal to the electrical signal via photodetectors was achieved. Till now, semiconductor materials have survived beyond its third generation, where the first generation is silicon-based devices, the second generation is GaAs-based infrared devices, and the third generation is devices based on wide bandgap semiconductors, such as group II-VI, III-V compounds, and newly emerging semiconductor materials [6]. Remarkable progress in high-performance photodetectors has been achieved. While in flexible ones, most of these semiconductor materials are limited to their intrinsic brittleness or incompatible high-temperature processes [7]. To obtain flexible photodetectors based on traditional semiconductor materials (silicon and group III-V, II-IV compounds), several strategies have been already demonstrated, such as reducing the film thickness to tens or hundreds of nanometers [8], integrating the serpentine shape or island-bridge structures with flexible substrates to achieve stress transfer from photoactive films to substrates [9–11]. Stretchable photodetectors can be obtained through these strategies, the performance is far from pretty, however. For, too-thin semiconductor films result in weak light absorption. Besides, the stretchable structures possibly cause additional complicated processes and easy destruction of the devices. For the next-generation flexible photodetectors, high performance and excellent mechanical flexibility should be achieved in a single device, simultaneously. To achieve this, photoactive films should have high light absorption coefficients to guarantee sufficient target light absorption with an ultrathin film thickness, for the mechanical property of

flexible devices is thickness dependent. Moreover, the process temperature for the fabrication of the devices must be limited to how flexible substrates can bear. This temperature is mostly below 250 °C [12], while it can be beyond 1000 °C for the processing of silicon and other semiconductors [13]. Developing novel semiconductor materials as candidates to process flexible photodetectors and improve the device performance is extremely urgent.

Metal-halide perovskites, a novel type of photosensitive semiconductor with excellent optoelectronic properties show great potential in the development of next-generation optoelectronic devices, such as solar cells, light-emitting diodes (LEDs), photodetectors, and lasers [14,15]. The efficiency of perovskite-based solar cells has exceeded the value of silicon-based ones in no more than ten years, while it took seventy years for silicon [16]. As shown in Fig. 1 [17], metal-halide perovskites generally refer to a type of crystals with the formula of ABX_3 in dimensions of three-dimensional (3D), 2D, 1D, and 0D, where A, B, and X represent monovalent cations ($CH_3NH_3^+$, $HC(NH_2)_2^+$, Cs^+ , etc.), divalent metal cations (Pb^{2+} , Sn^{2+} , etc.), and halide anions (Br^- , Cl^- , I^- , and their mixtures), respectively. An ideal crystallized perovskites structure is an octahedron, formed by a B ion coordinated with six X anions. The crystals of metal-halide perovskites are generally divided into three forms, including single crystals, nanocrystals, and polycrystalline films, where the latter two are widely used in flexible photoelectric devices. In comparison, polycrystalline films exhibit a lower exciton binding energy than the nanocrystals, pushing them into self-powered devices. While, the nanocrystals show higher photoluminescence quantum yields (PLQYs) than that of the polycrystalline, for defects lying in grain boundaries of polycrystalline films are easy to form, thus making nanocrystals more suitable for LEDs. However, the defects at the surface of nanocrystals also deteriorate the charge-carrier transport, lowering the PLQYs, device performance, and stability. Previous researches have demonstrated the properties of the nanocrystals and strategies for defects passivation [18,19]. Here, polycrystalline films possessing the merits of facial and low-cost processing, large optical absorption coefficient, tunable bandgap, high carrier mobility, long carrier diffusion length, and tolerance of defects [20–22],

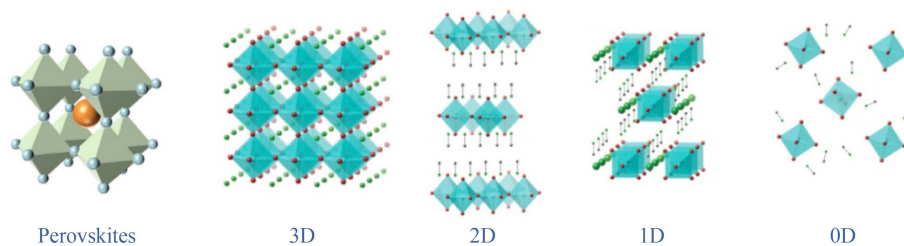


Fig. 1 Schematic illustration of perovskite with different dimensions (3D, 2D, 1D, and 0D) [17]. Reprinted with permission from Ref. [17] copyright@2023, Springer Nature.

are the focus here. Hopefully, polycrystalline films will offer wide opportunities for the fabrication of perovskite-based flexible photodetectors and make their development an attention in the field.

Generally, substrates, electrodes, semiconductor materials, and encapsulation layers are the four main compounds for photodetectors. As for substrates, thermal/chemical stability, transparency, and mechanical flexibility need to be considered for application in flexible photodetectors. So far, polymer materials, carbon cloth, fibers, and paper have been applied as the substrate materials. As for electrodes, conductivity, transparency, and flexibility are equally important, thus making indium-tin-oxide (ITO) not the best choice for its fragility [23,24]. Some other alternatives such as metal-based conductive networks, carbon-based conductive materials, and newly emerging 2D conductive materials have been also reported. Apart from substrates and electrodes, perovskite photoactive films are the most significant element of the photodetectors. Compared with the traditional inorganic semiconductor materials, perovskite polycrystalline films are intrinsically flexible with limited flexibility. Low-dimensional perovskites have been synthesized thus to enhance the performance of perovskite-based flexible photodetectors. Due to the instability of the perovskite materials, the encapsulation layers in devices play a significant role.

Having said above, the fabrication of flexible photodetectors involves the substrates, electrodes, perovskite films, and encapsulation layers. While, few reports focus on their processing strategies. Herein, a comprehensive summarization and discussion on the development of the perovskite-based flexible photodetectors is given. A brief introduction to the processing methods of the perovskite, the device architectures, and the performance parameters of the photodetectors are arranged first. For, the device architectures and fabrication methods of perovskite films affect the choices and processing of the substrates, electrodes, and encapsulation layers. Then, processing for the perovskite-based flexible photodetectors is attained the most of the attention, including the design of flexible substrates, soft electrodes, low-dimensional perovskites, conformal encapsulation, and elaborate device structures. Finally, typical applications of perovskite-based flexible photodetectors such as optical communication, image sensing, and health monitoring are also presented to show their potential significance. Challenges and future research directions in the field of perovskite-based flexible photodetectors are also proposed in the end.

2 Fabrication methods of perovskite

The methods of perovskite films fabrication roughly contain solution (Fig. 2 [25–30]) and vapor-based methods (Fig. 3 [31–35]), where solution-based ones

include spin coating, spray coating, slot-die coating, blade coating, ink-jet printing, etc., the vapor-based ones are composed of flashing evaporation, co-evaporation, sequential evaporation, chemical vapor evaporation, etc. [36]. In this section, a detailed presentation on the above-mentioned fabrication technologies will be given.

2.1 Solution-based methods

2.1.1 Spin coating

Spin coating is a method of film fabrication through the centrifugal force of liquids on the rotating substrates. For the fabrication of perovskite films, perovskite precursors are dissolved into the solvents first and spin-coated on the substrates. Most of the solvents evaporate during the rotating process, obtaining the crystalline films after an annealing process. As shown in Figs. 2(a) [25] and 2(b) [26], the spin coating methods involve one-step and multiple-step spin coating, since the perovskite materials are usually composed of multiple precursors. During one-step spin coating, organic/inorganic halide salts (MAX, FAX, CsX, etc.) and lead halide salts (PbX_2) are mixed and dissolved in the same solvent such as dimethyl sulfide (DMSO), chlorobenzene, or N,N-dimethylformamide (DMF). At times, to delay the crystal process for obtaining a homogeneous film or solve the problem that the precursors are not able to dissolve in a common solvent, organic/inorganic and lead halide salts may be dissolved in different or the same solvents and spin-coated on the substrate, sequentially. The spin coating method is not complex, where the components and thickness of the films can be easily tailored. However, this method causes serious waste on the precursors, and the quality of perovskite films decreases sharply with increasing areas, largely restricting large-scale and batch productions of perovskite-based devices [37]. To make things worse, the solubility of some precursors in the common solvents [38,39], or adhesion of the precursor solutions to substrates is rather low [40], especially for polymers, hampering its applications in these circumstances.

2.1.2 Spray coating

Spray coating as an ink-based method is suitable for the large-scale production of perovskite films compared with the spin coating method. The process diagram is presented in Fig. 2(c) [27], which involves a series of actions, such as production and atomization of the ink droplets, configuration of the droplets into a wet film, and film drying. Mechanisms of the atomization can be a high gas flow, ultrasonic stimulation, or cavitation of the ink [41,42]. Through spray coating, perovskite films can be manufactured automatically, rapidly, and with low

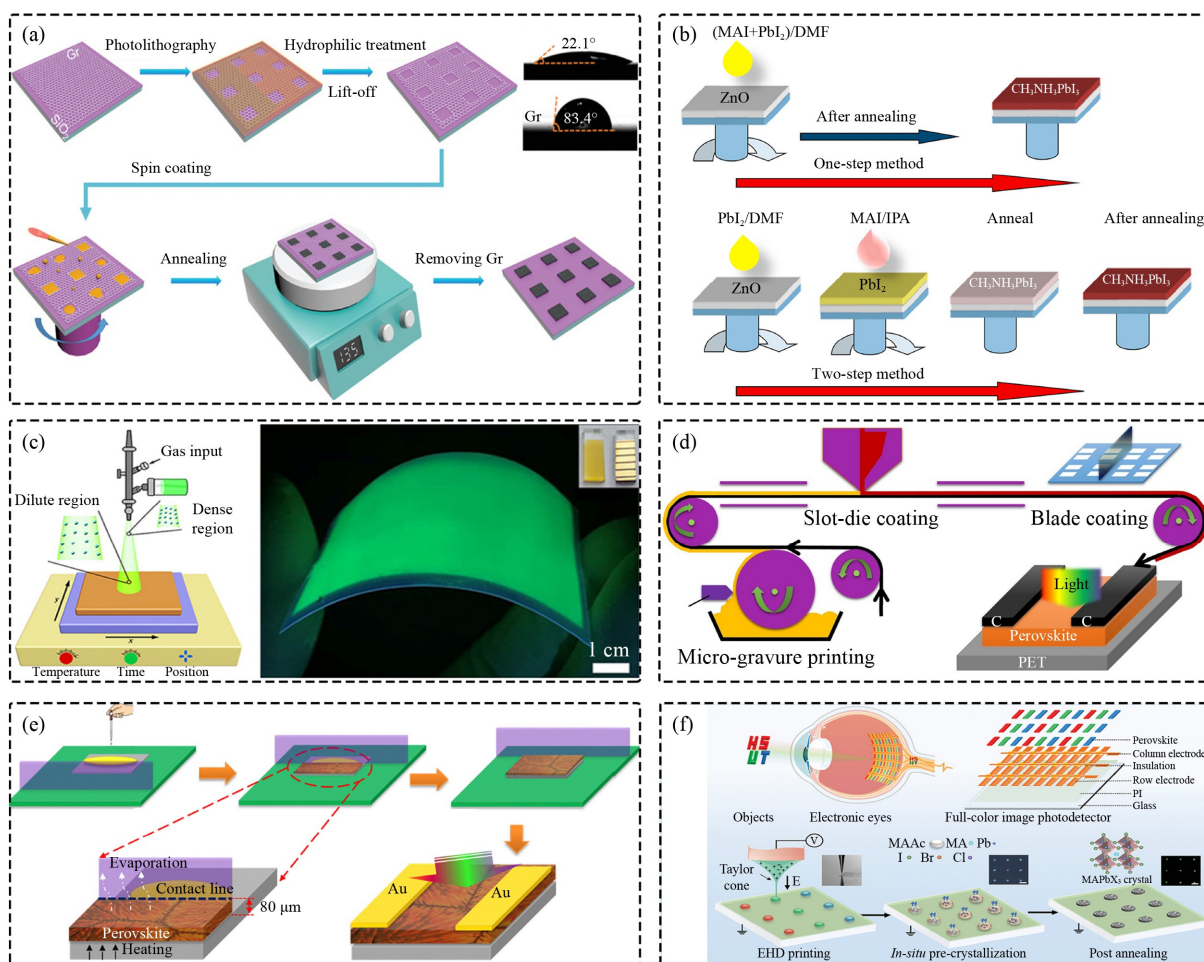


Fig. 2 Solution-based methods of (a) one-step spin coating [25], (b) multiple-step spin coating [26], (c) spray coating [27], (d) slot-die coating [28], (e) blade coating [29], and (f) ink-jet printing [30]. Reprinted with permission from Ref. [25], copyright@2019, Wiley-VCH. Reprinted with permission from Ref. [26], copyright@2020, Elsevier. Reprinted with permission from Ref. [27], copyright@2018, American Chemical Society. Reprinted with permission from Ref. [28], copyright@2019, Elsevier. Reprinted with permission from Ref. [29], copyright@2017, Elsevier. Reprinted with permission from Ref. [30], copyright@2021, Wiley-VCH.

material wastage. The thickness of the deposited perovskite films can be adjusted by the cycle times of spray coating, possibly sustained surface and bulk defects. This method also suffers from problems of precursor solubility and substrate adhesion.

2.1.3 Slot-die coating

In slot-die coating, perovskite precursors solution is squeezed out by required through a microfluidic metal die machine. As shown in Fig. 2(d) [28], substrates in the process were typically bendable materials such as polymer plastics. The head of the substrates was generally fixed on a roller to surpass the gravity force of the fluid. Wet films can be formatted during high-speed rotation, whose thickness is influenced by the geometry and speed of the roller [43]. Slot-die coating can deposit perovskite films in a large area with little precursor waste. And it is compatible with the roll-to-roll technology,

facilitating a preference for commercial large-area perovskite-based flexible photodetectors. However, the surface of films fabricated through this method shows relatively high roughness, limiting its usage in film deposition as modified layers.

2.1.4 Blade coating

Blade coating is a method of fabricating perovskite films through a blade moving across the substrates. As illustrated in Fig. 2(e) [29], the precursor solution was dropped onto a substrate, spread out, and scrapped into a thin film, then. A solid film can be obtained after drying. Preheating the substrates is an effective way to accelerate the process of blade coating and control the crystal quality of the films [44,45]. While, the method has a problem of imprecise control in the film thickness, and the chemistry of the solutions may change over time, making the quality of the films uncontrollable [36].

2.1.5 Ink-jet printing

Ink-jet printing is a method of controlling ink solutions through a microfluidic nozzle. During film fabrication, ink solutions are jetted out of the microfluidic nozzle under a pressure from thermal expansion, structure change, or electrical field. To promote efficiency, multiple nozzles are often used during the process. As shown in Fig. 2(f) [30], ink-jet printing has a distinct advantage over other methods of patterned film fabrication, which needs an additional etched process by other methods. It is also suitable for fabricating films on curved surfaces owing to its non-contact operation. In principle, this method can be used for printing any fluids or conductive materials. However, the occurrence of nozzle blockage restricts the specie and concentration of the inks [46,47].

2.2 Vapor-based methods

2.2.1 Flash evaporation

Flash evaporation is a vacuum-based method of film fabrication. As schematically presented in Fig. 3(a) [31], the perovskite materials were placed on a metallic heater or usual plate and converted to vapors under the heating

of electricity or a laser during processes. The vaporized perovskite materials are then condensed onto a substrate to form perovskite films under a high vacuum. The perovskite films obtained by this process are highly homogeneous and with minimal surface roughness, facilitating high-performance perovskite-based devices. Moreover, this method is scalable and controllable, making it compatible with industrial manufacturing. While compared with the solution-based methods, a high degree of halogen vacancy exists in the perovskite films, deteriorating the device performances (high noise, slow response, etc.) [48].

2.2.2 Co-evaporation

Co-evaporation is a more applicable vacuum-based method for film fabrication owing to its high maneuverability in chemical components. As shown in Fig. 3(b) [32], precursors, additives, or dopants were loaded in separate crucibles and transmitted into vapors once temperatures of the crucibles attain their sublimation temperatures. The deposition rates are in proportion to the working temperature, which can be used to tailor the stoichiometric ratios. The thickness of the final films can be controlled by adjusting the deposition time. The fabricated films through this process are denser and

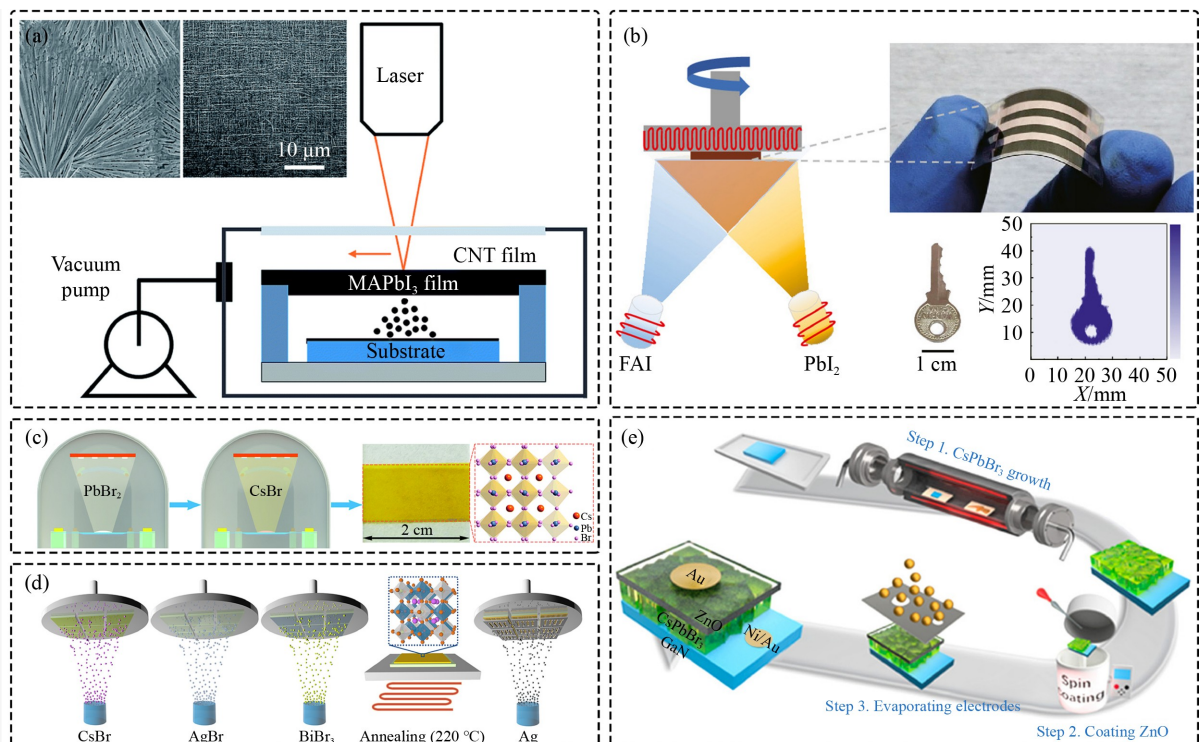


Fig. 3 Vapor-based methods of (a) flash evaporation [31], (b) co-evaporation [32], (c) two-step sequential evaporation [33], (d) multiple-step sequential evaporation [34], and (e) chemical vapor evaporation [35]. Reprinted with permission from Ref. [31], copyright@2017, Royal Society of Chemistry. Reprinted with permission from Ref. [32], copyright@2021, American Chemical Society. Reprinted with permission from Ref. [33], copyright@2021, American Chemical Society. Reprinted with permission from Ref. [34], copyright@2020, Royal Society of Chemistry. Reprinted with permission from Ref. [35], copyright@2017, American Chemical Society.

smoother. While, the separate deposition rates and precursors ratios need to be accurately standardized, making the control of the film's stoichiometry challenging [49].

2.2.3 Sequential evaporation

Sequential evaporation is another vacuum-based technology, involving separate deposition processes of multiple film layers, which diffuse and recrystallize under a heated condition. As shown in Figs. 3(c) [33] and 3(d) [34], the layers were deposited separately, making monitor of the deposition rates and chemical contents easier. Through the sequential evaporation process, high-quality perovskite films can be obtained without chemical alteration of the original perovskite materials. While the process is time-wasting and low-throughput. And, the quality of the films deteriorates with increased film thickness, restricted by inadequate diffusion [50].

2.2.4 Chemical vapor deposition

Compared with flash evaporation, co-evaporation, and sequential evaporation, chemical vapor deposition is achieved by placing multiple precursors in regions with different temperatures. The precursors can be in the form of solid or liquid. As depicted in Fig. 3(e) [35], inert gases such as nitrogen or argon gas were applied to carry vaporized precursors to the substrate. This technology has shown great potential in the synthesis of 2D perovskites (nanowires, nanorods, and nanosheets). Besides, this process avoids the utilization of high vacuum and annealing processes, reducing the cost and simplifying the preparation technology greatly. Films fabricated by this process are amorphous with flaws, which causes low charge-carrier transport [51].

2.3 Methods comparison

Through the summary above, perovskite thin films are commonly fabricated through solution and vapor-based methods. In this section, a comparison between the two types of methods will be analyzed in aspects of process complexity, process compatibility, and film quality.

For the solution-based methods, the preparation process is relatively simple without high vacuum or costly infrastructures, making them more cost-effective than the latter. Moreover, the throughput of films through solution-based methods is largely superior to the vapor-based ones. In a contrast, the vapor-based methods are comparatively slow due to their time-consuming pumpdown and small growth rate. Thus, the solution-based methods compatible with the commercial roll-to-roll technology will show great potential in large-area construction of flexible photodetectors.

As the aspect of process compatibility, substrate, film, and environment are three factors that need to be considered. In the process of solution-based methods, perovskite, small-molecule, and polymer films can be fabricated. While, the adhesion between the films and substrates is weaker, limiting the choice of substrate materials and resulting in a device performance decline. Through vapor-based methods, films, especially ultrathin ones can be grown on various substrates. A significant benefit of vapor-based methods is their absence of toxic solvents, which is environmentally friendly, while the solution-based ones suffer from the usage of organic solvents or antisolvents, such as DMF, DMSO, and chlorobenzene. However, polymer films which are widely used as passivation or encapsulation layers in flexible photodetectors can be scarcely finished through vapor-based methods. Moreover, the chemistry of perovskite films can be tailored easily, which is complicated for vapor-based methods.

Vapor-based methods have been well-known and widely used in the coating and semiconductor industry. The films exhibit a salient advantage of the sublimed materials' intrinsic purity over that fabricated by the solution-based methods. And, the films obtained show homogeneous, smooth, and dense surfaces with greater adherence to the substrates, whose quality can be maintained over a large area or an ultrathin film thickness with high precision. While the vapor-based methods need an additional periodical calibration to properly maintain the deposition rate and precursor ratio.

3 Architectures and performance parameters of photodetectors

3.1 Architectures of photodetectors

Photodetectors, converting external light illumination into an electronic signal, have been fundamental devices in academia and industry. Various types of photodetectors have been developed and applied to a variety of circumstances, such as imaging, spectroscopy, and communications. In general, the wavelengths of external lights range from X-ray, ultraviolet, visible, and infrared lights, and the photodetectors can respond to a single (narrowband photodetectors) or multiple (broadband photodetectors) wavelength bands. From the aspect of device structures and working mechanisms, the photodetectors are roughly divided into photodiodes, photoconductors, and phototransistors [52]. As shown in Fig. 4, photodetectors here are divided according to the relative position between the electrodes, where the photodiodes and lateral photoconductors are two-terminal devices with vertical and lateral configurations, respectively. The phototransistors are three-terminal devices with electrodes named a drain, source, and gate [53,54]. Besides, there is another

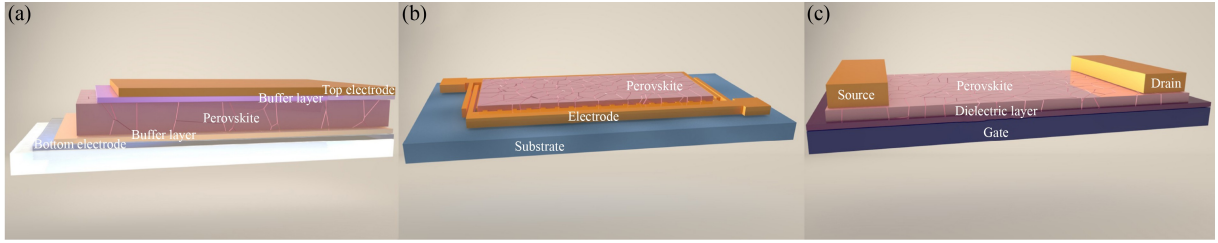


Fig. 4 Schematic illustrations of (a) photodiodes, (b) photoconductors, and (c) phototransistors.

classification way, where the photodetectors are divided by their working principles, containing photodiode, vertical and lateral photoconductor, and phototransistor [55,56]. For the fabrication of flexible perovskite photodetectors, the device performance, flexibility, fabrication process, and cost are influenced by the device structures.

In a typical photodiode, the functional film is sandwiched by the top and bottom electrodes absorbing incident light and producing e-h pairs [57]. The e-h pairs are then separated by built-in electric fields generated from the vertical p-n, p-i-n, or Schottky junctions owing to the low excitons binding energy of perovskite [58]. When a photodiode operates in the photovoltaic mode, a reversed electric field is applied to facilitate the separation. The separated e-h pairs are then drifted toward the respective electrodes through a narrow electrode spacing defined by the thickness of perovskite films. The additional reverse bias voltage can increase the carriers' collection efficiency. However, the lack of an internal gain mechanism induces a low external quantum efficiency (EQE) below 100% due to the absence of charge injections under reverse bias voltages with blocking/rectifying contacts [59].

Compared with photodiodes, lateral photoconductors with electrodes contacted with photoactive films in symmetrical or asymmetrical Ohmic states can be prepared and integrated, facilely. Moreover, photoconductors can obtain a high gain and EQE benefiting from the unbalanced electron and hole transportation, where the electron or hole is trapped and the other one can recirculate before recombination [60]. A driving voltage is necessary for devices with symmetrical electrodes to separate the photogenerated e-h pairs and transport the carriers [61]. For devices with asymmetrical electrodes, a carrier driving force can be generated, which is decided by the difference in the work function of the metal electrodes. Compared with photodiodes, flexible photoconductors can be fabricated without using transparent electrodes, broadening the choice of electrode materials. However, lateral devices (photoconductors and phototransistors) suffer from a high driving voltage and a long response time due to the wide electrode spacing [62]. Dark currents in photoconductors with Ohmic electrode contacts are relatively high under a bias voltage, leading

to a low detectivity and a narrow linear dynamic range (LDR).

Phototransistors are lateral devices composed of a conductive channel, a thin dielectric layer, and three electrodes, which are treated as a combination of photodiodes and field-effect transistors (FETs). Similar to the typical FETs, the charge concentration in phototransistors can be tailored by changing the gate voltage between the semiconductor and the gate electrode, thus realizing signal amplification [63]. Compared with photodiodes and photoconductors, phototransistors enable a relatively low dark current in the depletion regime and a high gain with a bias voltage under light illumination, overcoming the trade-off between low dark currents and high gains to some extent. Nevertheless, phototransistors suffer from complicated fabrication processes and low response speed.

3.2 Performance parameters of photodetectors

To evaluate the performance of photodetectors comprehensively, EQE, responsivity (R), specific detectivity (D^*), on/off ratio, response time, LDR, and photoconductive gain (G) need to be considered. Flexibility and stability as critical properties of flexible devices are particularly significant [64]. The comparison between the device structure and performance parameter is listed in Table 1 below.

3.2.1 External quantum efficiency

EQE also known as incident photon-to-current efficiency (IPCE), is a distinct parameter to evaluate the ability to convert photons into charges. It represents the ratio of photo-induced electrons/holes to the incident light photons, obeying the following equation:

$$\text{EQE} = R \frac{hc}{q\lambda}, \quad (1)$$

where h , c , and q are constants, representing Planck's constant, speed of light, and elementary electron charge, respectively, and λ is the wavelength of the incident light. One can conclude that the EQE is proportional to the responsivity.

Table 1 Comparison between the device structure and performance parameter

Device structure	EQE	R	D^*	Response time	G	LDR	Driving voltage	Photocurrent/dark current
Photodiode	$\leq 100\%$	Low	High	Short	Small	Large	Low (~ 0)	Low
Photoconductor	$> 100\%$	High	Low	Long	Large	Narrow	High	High
Phototransistor	$> 100\%$	High	Low	Long	Large	Narrow	High	High

3.2.2 Responsivity

R is another parameter to indicate the photoelectric performance of photodetectors, defined as the ratio of photo response (photocurrent or photovoltage) to the incident light intensities. It can be calculated by the following equation:

$$R = \frac{J_{\text{photo}}}{P_{\text{in}}} = \frac{I_{\text{light}} - I_{\text{dark}}}{P_{\text{in}} S}, \quad (2)$$

where I_{light} and I_{dark} are the currents under light and dark conditions, J_{photo} is the photocurrent density, S is the effective area of photodetectors, and P_{in} is the power density of the incident light.

3.2.3 Specific detectivity

Detectivity (D) represents the photodetecting sensitivity of a photodetector from environmental noise, expressed by the inverse of the noise equivalent power (NEP). It will be re-defined as D^* when the NEP is normalized by the device area (S) and the bandwidth (Δf) through square root calculation. It can be derived from the following equation:

$$D^*(\text{Jones}) = \frac{(S \Delta f)^{1/2}}{\text{NEP}} = \frac{R}{\sqrt{2qI_{\text{dark}}/S}}. \quad (3)$$

3.2.4 On/off ratio

Besides the D^* , the on/off ratio also reflects the sensitivity of photodetectors to light signals, which can be calculated by the ratio of photocurrent (I_{light}) to dark current (I_{dark}) under the same conditions. The dark current is a key parameter for photodetectors in real applications since it decides how weak light can be detected [65,66]. A relatively high dark current will significantly increase the power consumption and complicate the readout circuits [67,68]. The photocurrent mainly depends on the ability of photoelectric conversion and charge transport efficiency of the photoactive films [69]. A high on/off ratio represents a high contrast between the desired signal and the noise signal. To increase the ratios, enhancing the photocurrent and/or suppressing the dark current are effective ways.

3.2.5 Response time

Response time is an indicator of the response speed of

photodetectors to the incident lights in the time domain. A short response time means a fast response speed, which is especially significant in applications of light communication, ultrafast light detection, and image sensors. The response time generally consists of the rising time (τ_{rise}) and falling time (τ_{fall}), closely connected with the processes of charge transfer and collection. τ_{rise} and τ_{fall} are defined as the time for the currents rising from 10% to 90% of their maximum value under light illumination, and the time for the current decaying from 90% to 10% of their maximum value after the removal of the incident lights, respectively [70].

3.2.6 Linear dynamic range

LDR reflects the range over which the photocurrent or the photovoltage is linear to the incident light powers in logarithmic graphs. It also indicates the reliable signal range. The value of LDR can be calculated by the following equation [71,72]:

$$\text{LDR} = 10 \lg \frac{P_{\text{max}}}{P_{\text{min}}} \text{ or } \text{LDR} = 20 \lg \frac{P_{\text{max}}}{P_{\text{min}}}, \quad (4)$$

where P_{max} and P_{min} are maximum and minimum detectable light densities in the linear range, respectively. Values of LDR can be obtained by intensity-dependent photocurrent measurements. In principle, P_{min} is highly influenced by the noise, and P_{max} is synergistically affected by the processes of carrier extraction and recombination.

3.2.7 Gain

Gain (G) is defined as the number of photogenerated charge carriers per incident photon, which is characterized by the ratio of the carrier lifetime (τ_{lifetime}) to the carrier transit time (τ_{transit}).

$$G = \frac{\tau_{\text{lifetime}}}{\tau_{\text{transit}}} = \frac{\tau_{\text{lifetime}}}{d^2/(\mu V)}, \quad (5)$$

where d is the channel length of photodetectors, V is the bias voltage, and μ is the carrier mobility. Once the lifetime of the carriers is longer than the transit time, a gain G will be therefore generated.

3.2.8 Flexibility and stability

Flexibility as an indispensable factor must be considered for flexible photodetectors. It is closely related to the

substrates, functional films, electrodes, and encapsulation layers of devices. Herein, the functional films are specified as perovskite, which can be considered as a mechanically “soft” material compared with conventional semiconductors (silicon and germanium). For perovskite-based flexible photodetectors, the thickness, morphology of the perovskite, and its contacting quality among different layers also affect the device’s flexibility.

Stability is another significant parameter in practical applications, evaluated by the maintenance of the electrical parameters (photocurrent or dark current) in the time domain. Besides this, it also contains the aspect of mechanical stability for flexible photodetectors, which is defined as the ability to maintain electrical properties under different test conditions including periodic bending at a set angle/radius, folding, and stretching.

4 Processing for flexible photodetectors

As for flexible optoelectronic applications, photodetectors need to be mechanically flexible and stretchable to attach to curved surfaces, apparel fabric, or human skin [54]. To be intrinsically flexible, core elements of the photodetectors including substrates, electrodes, functional films, encapsulation layers, and other electronic parts in the system should be selected and designed elaborately. Besides these, low-dimensional perovskites (0D, 1D, and 2D) and various device structures to enhance flexibility have been explored and yielded great success. As schematically concluded in Fig. 5, perspectives of flexible substrates, soft electrodes, conformal encapsulation, low-dimensional perovskite, and elaborate device structures will be discussed.

4.1 Flexible substrates

Flexible substrates as the fundamental element decide the flexibility of photodetectors mostly, whose choice depends on the device structures. For photovoltaic-type photodetectors, lights illuminate from the bottom of the devices, requiring substrates to be transparent. For the photoconductor- or phototransistor-type devices, the transparency of substrates seems beside the point. This part fixes attention on various types of flexible substrates: polymers, carbon cloth, fibers, and paper.

4.1.1 Polymer

Polymers are widely used as substrates in flexible photodetectors for their easy access, precisely controlled thickness and shape, intrinsic flexibility, and possible fabrication for large-scale production [73]. As discussed above, light transmittance is a precondition for devices with lights illuminated from the bottom side. Perovskites fabricated through a solution or vapor-based methods involve the utilization of organic solvents or high-temperature annealing processes, making temperature tolerance, solvent resistance, and dimensional stability of the polymer substrates significant. Thus, light transmittance, dimensional stability, temperature tolerance, solvent resistance, elastic modulus, etc. need to be considered simultaneously for the choice of polymers [74]. As detailed in Table 2, the parameters of commonly used polymer materials are concluded to provide principles for substrate choices.

Commonly used polymer substrates are listed in Fig. 6 [75–78]. In Figs. 6(a)–6(c) [75–77], flexible photodetectors in laboratory fabrication were mostly based on polyethyleneterephthalate (PEN) [79], polyethylene terephthalate (PET) [80,81], and PVDF (polyvinylidene fluoride) [82]. To enhance the flexibility of the polymers,

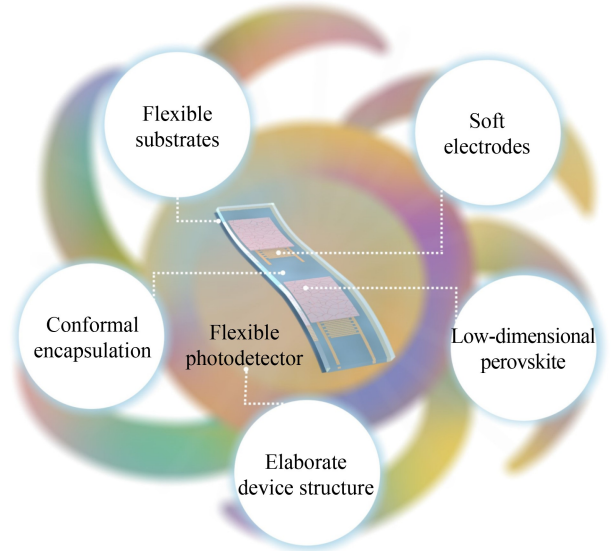


Fig. 5 Processing for flexible perovskite photodetectors.

Table 2 Properties of typical polymer materials

Polymer	Light transmittance/%	Dimensional stability	Temperature tolerance/°C	Solvent resistance	Elastic modulus/MPa
Polyethyleneterephthalate (PEN)	87.0	Well	120	Well	6000
Polyethylene terephthalate (PET)	90.4	Well	79	Well	4000
Polyvinylidene fluoride (PVDF)	25–30	Well	150	Well	1400
Polyimide (PI)	30–60	Well	280	Well	500
Polydimethylsiloxane (PDMS)	93	Fair	260	Fair	150
Poly(methyl methacrylimide) (PMMA)	92	Fair	100	Fair	6500

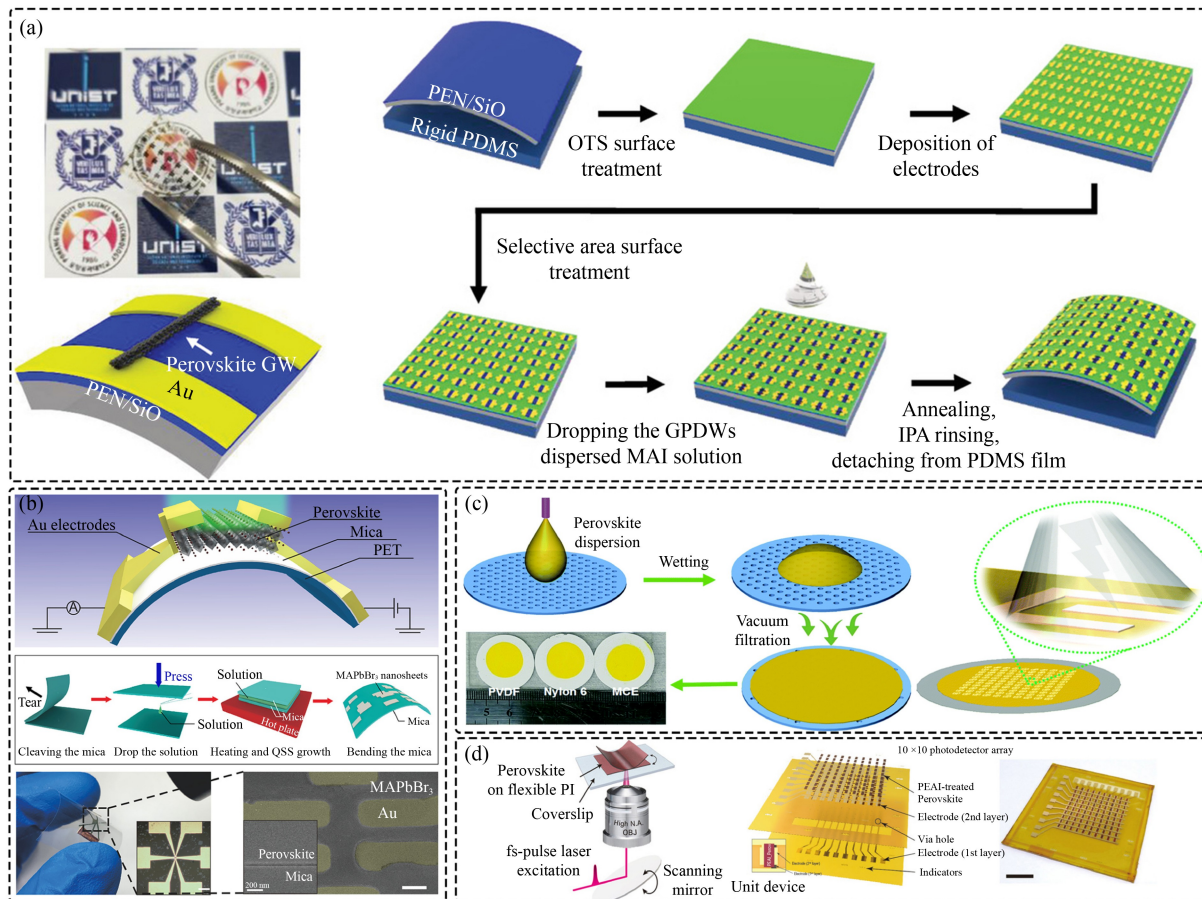


Fig. 6 Perovskite photodetectors on polymer substrates of (a) polyethylenenaphthalate (PEN) [75], (b) polyethylene terephthalate (PET) [76], (c) polyvinylidene fluoride (PVDF) [77], and (d) polyimide (PI) [78]. Reprinted with permission from Ref. [75], copyright@2017, Wiley-VCH. Reprinted with permission from Ref. [76], copyright@2020, American Chemical Society. Reprinted with permission from Ref. [77], copyright@2019, Royal Society of Chemistry. Reprinted with permission from Ref. [78], copyright@2020, American Chemical Society.

a PET substrate was structured by laser, releasing the performance degradation greatly during operations [83]. The mechanism of this flexibility enhancement is that the structured PET substrate with micro/nanostructures makes the stress distributed inside itself, while it tends to be concentrated on the surface of the flat ones. Despite the incredible progress of perovskite-based flexible photodetectors on polymer substrates, most of the substrates suffer from a low glass transition temperature, restricting the device's processing temperature below 150 °C. While, the temperatures may be higher than 200 °C [33] or even attain 300–400 °C [84] in the vapor-based methods, causing incompatibility with the polymer substrates. PI film as an optimum substrate material can bare a high temperature of 400 °C and operate at a temperature of 330 °C for a long time. As presented in Fig. 6(d) [78], perovskite photodetector arrays were constructed on flexible PI/coverslip composite substrates. Then, the flexible devices on PI films were peeled off from coverslips aimed by an fs-pulse laser, which can avoid the destruction of the etching solvents to the perovskite films.

4.1.2 Carbon cloth

Carbon cloth has superior flexibility and higher temperature tolerance (> 500 °C) than polymers. It can also serve as both a flexible substrate and conductive electrode, simplifying the fabrication processes to a great extent. As shown in Fig. 7 [85], perovskite-based flexible photodetector was constructed on carbon cloth, with performance degraded negligibly after bending for several tens of cycles and at an extreme bending angle of 180°.

4.1.3 Fiber

Fibers are also promising candidates for developing flexible photodetectors owing to their intrinsically flexible structures, among which the yarn, carbon, and polymer fibers were explored, as shown in Fig. 8 [86–88].

Fibrous yarn bundles are widely used as templates to fabricate perovskite films with controlled morphology and dimensionality owing to their high flexibility and

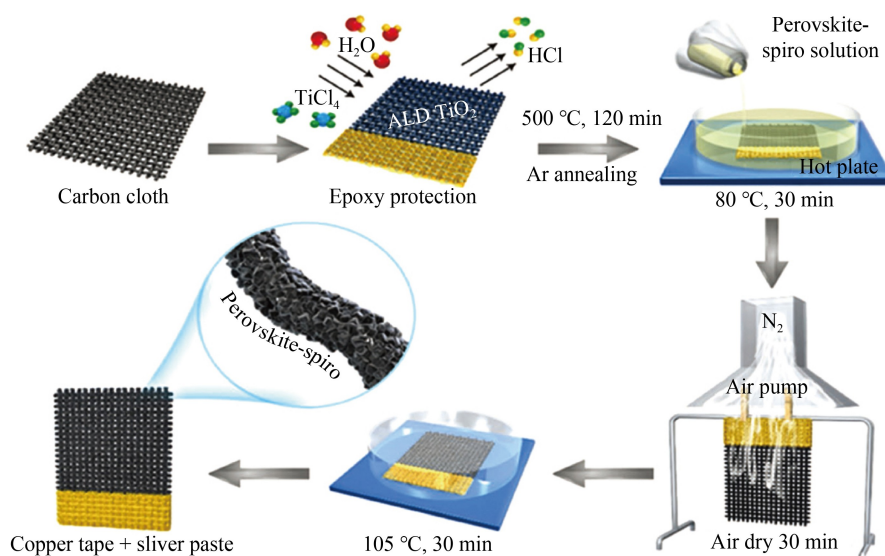


Fig. 7 Fabrication process of carbon cloth-based flexible photodetectors [85]. Reprinted with permission from Ref. [85], copyright©2017, Wiley-VCH.

easily knitted into various patterns. Aimed by the capillary force of the perovskite precursor solutions and “quasi-spring” like networks, flexible photodetectors were constructed with the process depicted in Fig. 8(a) [86]. The knitted fibrous yarn bundles in the “quasi-spring” like network showed excellent elasticity and stress elimination like cushions, benefitting the device’s excellent work stability with ignorable photocurrent attenuation after 200 bending cycles or under a twisted state at 180°.

Devices fabricated on yarn bundles need additional two electrodes due to their intrinsic insulativity. Carbon fibers can serve as fibrous substrates and conductive electrodes, simultaneously. As shown in Fig. 8(b) [87], a CuO-Cu₂O-Cu wire was regarded as the device substrate with perovskite-TiO₂-carbon fiber deposited on the surface of the wire in a double-twisted structure. The devices demonstrated excellent flexibility and bending stability, without response speed degradation at an extreme bending angle of 90°.

These fiber-based photodetectors show a twisted structure, where one fibrous electrode is incorporated with perovskite and entwined by another fiber electrode. The solution-based methods may make no sense for the fabrication of fiber-based flexible photodetectors. Polymer fibers can be solution-processed giving a possibility of mixing the precursors of perovskite and polymers in advance and constructing fibrous morphology then. As shown in Fig. 8(c) [88], composite nanofibers of polymer/perovskite were electrospun on a rubbery PDMS substrate. Through this strategy, polymer fibers with various shapes can be obtained from the precursor solution directly.

fabrication of flexible photodetectors owing to its adequate availability, low cost, mechanical flexibility, and biocompatibility [89]. Compared with polymers and fibers, paper substrates show better adhesion between substrates and perovskite precursors for their porous structure, benefiting paper as a suitable substrate material for both solution and vapor-based flexible photodetectors [90,91]. As shown in Fig. 9 [92–94], precursors were drop-coated on a paper directly, which will be absorbed into the micropores/nanopores quickly driven by the unique capillary force of papers (Fig. 9(a)) [92]. Moreover, perovskite-based flexible photodetectors were also constructed on paper substrates through a dual-source physical vapor deposition method and a brushing-coating method, with processes depicted in Fig. 9(b) [93]. The two types of devices equipped almost a similar performance, demonstrating paper substrates are versatile substrate materials for the fabrication of high-performance perovskite-based photodetectors.

In addition, the bendability of paper is superior to that of polymers. The plasticity of the 3D structure is also better than that of the fibers. These all bring new design inspirations. For instance, an origami perovskite photodetector was demonstrated as shown in Fig. 9(c) [94], in which pencil trace and common printing papers were used as the graphite electrodes and substrates, respectively. Besides excellent mechanical flexibility and durability, salient spatial recognition ability was also achieved benefitting from the ingenious origami structure.

4.2 Soft electrodes

4.1.4 Paper

Paper is another commonly used substrate for the

Traditional metallic materials such as silver, gold, and aluminum are widely used as electrodes in photodetectors

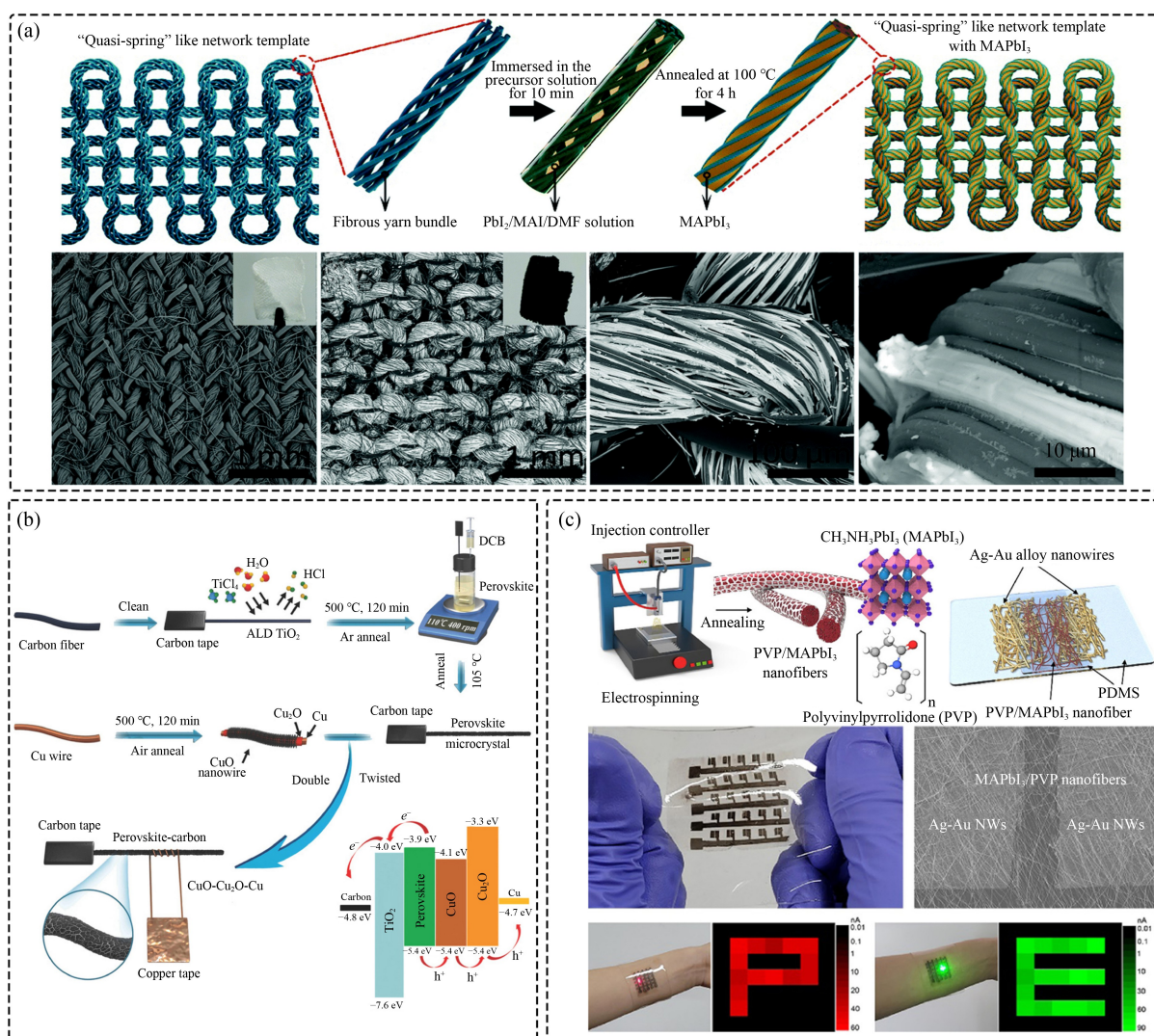


Fig. 8 Fabrication processes and characteristics of (a) yarn [86], (b) metal [87], and (c) polymer fiber-based flexible photodetectors [88]. Reprinted with permission from Ref. [86], copyright@2019, Royal Society of Chemistry. Reprinted with permission from Ref. [87], copyright@2018, Wiley-VCH. Reprinted with permission from Ref. [88], copyright@2022, American Chemical Society.

owing to their easy access by vacuum deposition and superior compatibility with most substrate materials. While they suffer from poor light transmittance. ITO and fluorine-doped tin oxide (FTO) with low square resistance and high transparency are regarded as candidates for electrode materials to solve the above problem. These materials are all inherently brittle, limiting their widespread use in flexible devices [23,24]. To overcome the bottleneck, stretchable structures were designed to decorate the metallic materials, such as spiral snake-like structures [95], island-bridge structures [96], and wrinkled structures [97]. These structures are most fabricated on a planner surface to enhance the stretching ability, which may fall failure during folding or bending. Metal-based conductive networks, carbon-based conductive materials, and newly emerging conductive materials have received focused attention recently, potentially

balancing light transmittance, conductivity, and mechanical flexibility.

4.2.1 Metal-based conductive networks

Mature fabrication technologies such as ink-jet printing, electrostatic spinning, and 3D printing are limited in synthesizing metal-based conductive networks directly due to the high melting point of metals. A method of combining mask-based deposition methods and a lift-off process was ingeniously designed, where polymer networks were constructed through ink-jet printing, electrostatic spinning, or 3D printing first. Then, the polymer masks were constructed on the top surface of metal films and used as the etching masks, or on the substrates to serve as reverse pattern masks. Figure 10 [98,99] shows two types of metal-based conductive

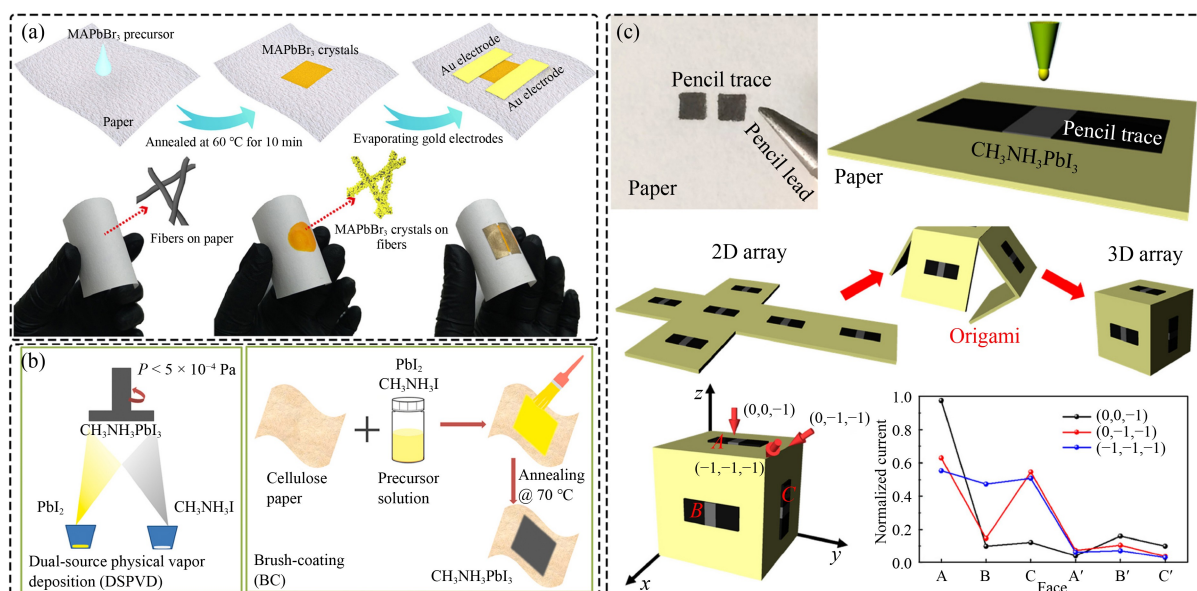


Fig. 9 Fabrication process of paper-based flexible: (a) photoconductor [92], (b) photodiode [93], and (c) cubic photodetectors [94]. Reprinted with permission from Ref. [92], copyright@2021, American Chemical Society. Reprinted with permission from Ref. [93], copyright@2021, Elsevier. Reprinted with permission from Ref. [94], copyright@2017, American Chemical Society.

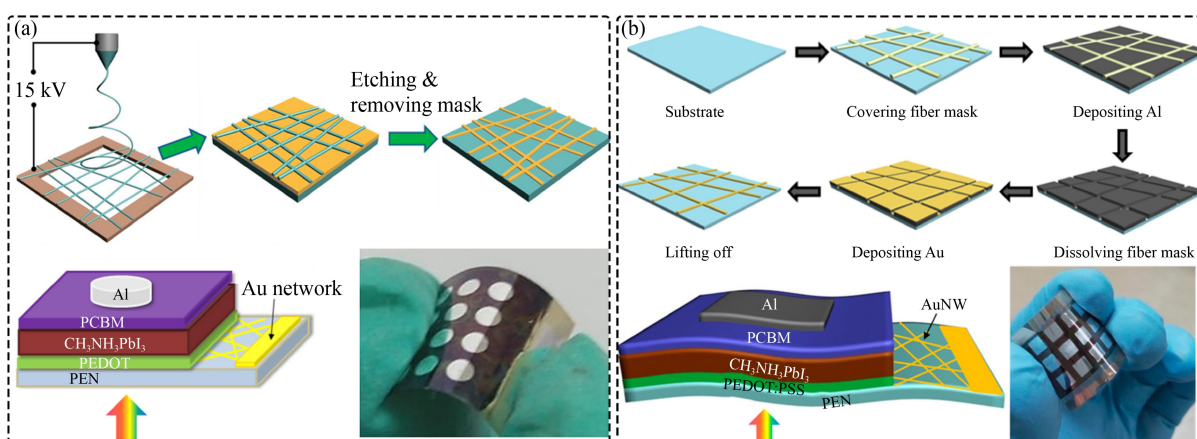


Fig. 10 (a) Direct [98] and (b) indirect etching processes for fabrication of metal-based networks [99]. Reprinted with permission from Ref. [98], copyright@2016, American Chemical Society. Reprinted with permission from Ref. [99], copyright@2018, American Chemical Society.

networks and their fabrication process. As shown in Fig. 10(a) [98], a polymer network was deposited on the surface of a gold film through electrostatic spinning, based on which the part of the metal film without protection was exfoliated, obtaining a metal network after the removal of the polymer masks. In this process, peeling off the metal films and doing no damage to the polymer itself is a key point in deciding the final result. While searching for proper etching solvents seems to be difficult. To improve this, electrospinning polymer networks on the top surface of substrates as reverse pattern masks as shown in Fig. 10(b) [99]. An intermediary mask with materials of Al, Ni, etc. was manufactured based on the polymer mask. The solvents

of water/HCl and organic solutions were used to dissolve the intermediary mask and polymer masks, respectively.

4.2.2 Carbon-based conductive materials

Carbon-based conductive materials such as graphite and carbon nanotubes are also candidates for transparent electrodes owing to their proper transparency, excellent conductivity, and high stability, where are concluded in Fig. 11 [100–103]. Generally, high-quality graphene films are grown on copper foils through a chemical vapour deposition (CVD) progress, with a spin-coated PMMA layer to assist the transfer progress. After etching the copper foil, composite films of graphene and PMMA

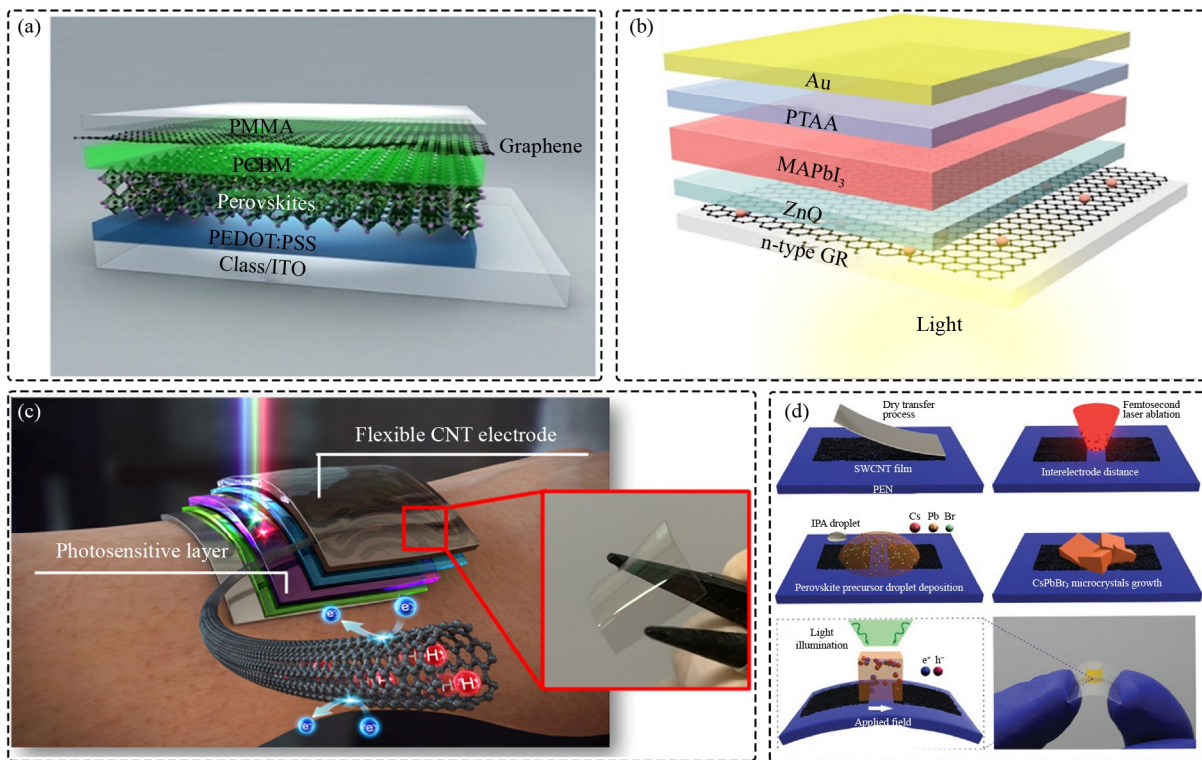


Fig. 11 Fabrication processes and device structures of flexible photodetectors with (a) top graphene electrode [100], (b) bottom graphene electrode [101], (c) top carbon nanotube electrode [102], and (d) bottom carbon nanotube electrode [103]. Reprinted with permission from Ref. [100], copyright@2021, IOP Publishing. Reprinted with permission from Ref. [101], copyright@2019, American Chemical Society. Reprinted with permission from Ref. [102], copyright@2021, Elsevier. Reprinted with permission from Ref. [103], copyright@2022, Wiley-VCH.

with a vertically stacked structure can be obtained. As shown in Figs. 11(a) [100] and 11(b) [101], the transferred graphene/PMMA was applied as the top and bottom transparent electrodes, respectively. Similarly, randomly oriented carbon nanotubes with high purity and long nanotube bundle length were also synthesized through an aerosol CVD method. Carbon nanotubes in the form of power were then dissolved into the dispersion solution or collected by nitrocellulose filters, serving as the flexible transparent electrodes as depicted in Figs. 11(c) [102] and 11(d) [103].

4.2.3 Two-dimensional conductive materials

One property of the perovskite materials is their tunable bandgaps. Traditional metallic materials such as Au, Ag, and Pt. are usually with high work functions, causing high Schottky barriers between the perovskite film and electrodes due to their mismatch of work functions. This Schottky barrier results in ineffective charge carrier transport, reducing the device's performance significantly. Newly-emerging two-dimensional $\text{Ti}_3\text{C}_2\text{T}_x$ (MXene) (Fig. 12 [104,105]) with adjustable work functions (1.6–6.2 eV), excellent conductivity, and high transmit-

tance has received research attention in flexible electronic devices. Compared with CVD-processed carbon-based materials, MXene is commonly fabricated through top-down techniques containing spin-coating and laser-scribing, which can maintain the properties of the initial materials. As demonstrated in Fig. 12(a) [104], the MXene with a coiled shape was spray coated on a common paper substrate by an elaborately selected cold working process. Similarly, the MXene was spin-coated on a hydrophilic silicon substrate with a laser-scribing process to pattern the electrodes as shown in Fig. 12(b) [105].

4.3 Conformal encapsulation

Conformal encapsulation is significant for the long-time operation of perovskite-based flexible photodetectors, which can isolate the perovskite film from moisture, oxygen, and thermal [106,107]. It is also effective to solve the problem of lead leakage [108]. Materials used for encapsulation need to do no damage to the under-layer perovskite and possess excellent moisture/oxygen resistance, high transparency, and mechanical flexibility. The methods of conformal encapsulation for perovskite-

based flexible devices are roughly divided into single-layer (Fig. 13 [109,110]) and multilayer encapsulation (Fig. 14 [111]).

4.3.1 Single-layer encapsulation

In the laboratory, single-layer encapsulation is the most

commonly used method, which can be carried out by depositing a capping layer on the top surface of the device [112,113]. The effect of encapsulation is decided by the encapsulation materials and processing technology. As for the materials, polymers, and inorganic metal oxides have been applied for encapsulation. Polymers are widely used for their high throughput production and

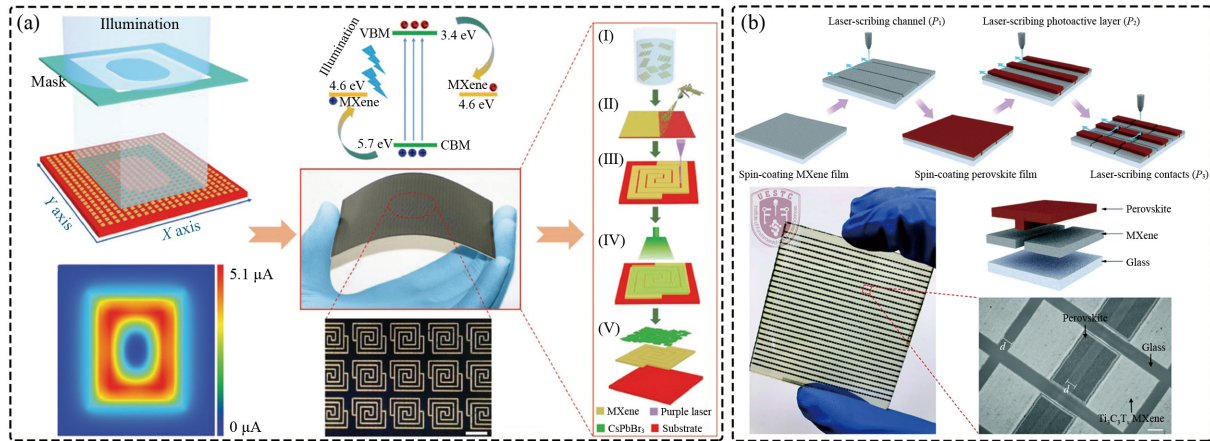


Fig. 12 (a) Fabrication processes and (b) device structures of flexible photodetectors with MXene electrodes [104,105]. Reprinted with permission from Ref. [104], copyright@2019, Wiley-VCH. Reprinted with permission from Ref. [105], copyright@2020, Royal Society of Chemistry.

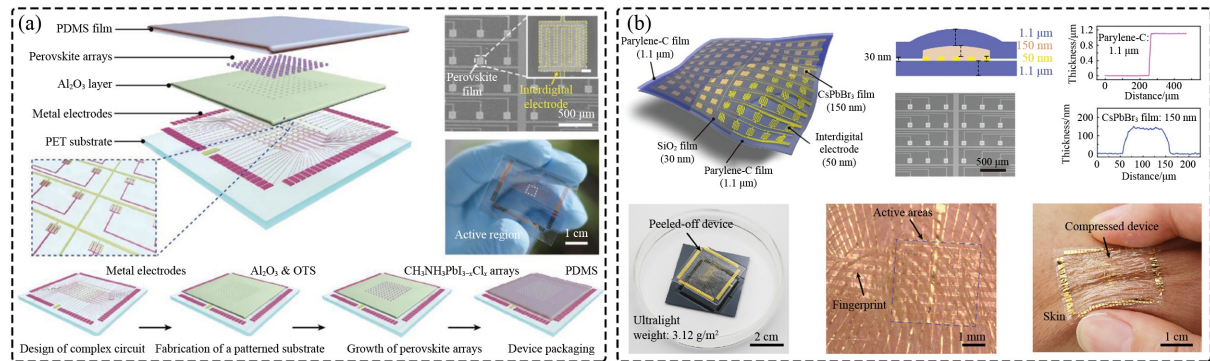


Fig. 13 Flexible photodetectors encapsulated by polymers of (a) polydimethylsiloxane (PDMS) [109] and (b) parylene-C film [110]. PET: polyethylene terephthalate. Reprinted with permission from Ref. [109], copyright@2018, Wiley-VCH. Reprinted with permission from Ref. [110], copyright@2021, Wiley-VCH.

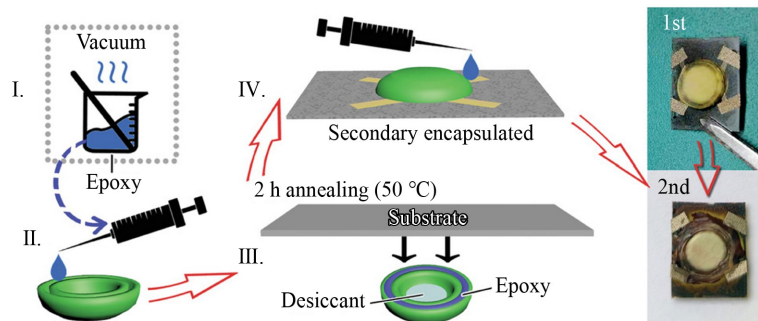


Fig. 14 Flexible photodetectors encapsulated with a composite of shell, epoxy, and desiccant [111]. Reprinted with permission from Ref. [111], copyright@2022, Wiley-VCH.

barrier ability for water and oxygen. As shown in Fig. 13(a) [109], PDMS was spin-coated on the top surface of the perovskite photodetector array as an encapsulation layer. Other polymers such as PMMA [114] and silica aerogels [115] have also been deposited to achieve encapsulation of perovskite. The thicknesses of the polymer films are controlled by the rotation speed. A thick polymer layer may benefit the encapsulation while worse the device flexibility. The perylene-C film was deposited through special CVD equipment [116], which can attain an excellent encapsulation effect with a far thinner thickness than that of other polymer materials. As shown in Fig. 13(b) [110], the perylene-C films were applied as the substrate and encapsulation layer, simultaneously, between which the devices showed high flexibility and water/oxygen resistance.

Besides the polymer materials, inorganic metal oxides are also considered potential materials, since dense films can be deposited through a vacuum or vapour-based methods. Among them, AlO_2 [117] and HfO_2 [118] deposited by atomic layer deposition (ALD), and SiO_2 [119] processed by plasma enhanced chemical vapour deposition (PECVD), etc. have demonstrated excellent performance in encapsulation. These inorganic materials with high dielectric constant were also used as insulating layers in photoelectric devices owing to their excellent insulativity with thin film thickness.

4.3.2 Multilayer stacked encapsulation

Single-layer encapsulation through polymers or inorganic metal oxides is intrinsically defective for the particles or defects in the materials themselves. Various issues may break the protective barrier of the encapsulation layer and harm the underlying perovskite-based devices, such as edge permeation, intrinsic defects of the films, and film density [120]. Multilayer stacked encapsulation is an effective way to address these problems, potentially.

Polymer materials used for single-layer encapsulation are porous usually, causing serious surface permeation due to the surface film defects. Fluorinated silica was inducted into the porous PDMS foam to improve the film quality, and the devices showed salient stability in moisture, heat, and irradiation environment benefitting the superhydrophobic and thermal insulativity of the fluorinated silica [121]. Similarly, ethylene-vinyl acetate (EVA) stacked with PI films has also been used as encapsulation materials and designed to shift the location of the neural axis to the ITO electrode [122]. A spray-coated organic-inorganic composite film with polystyrene (PS)-4033/PS-4033- SiO_2 was also used as the encapsulation layer, extending the device's lifetime by about 10 times that of the bare ones [123]. With the assistance of 3D printing technology, a new encapsulation layer containing a printed flexible UV-curable resin shell, AB

epoxy, and a desiccant sheet was demonstrated, with the process of encapsulation presented in Fig. 14 [111]. The shell equipped itself with ring groves to hold the AB epoxy and avoid squeezing. The epoxy with the property of self-healing prevented cracks in the materials or interface segregation between the encapsulation layer and flexible substrate [124]. This strategy effectively avoided the absence of edge/surface permeation, film defects, etc.

4.4 Low-dimensional perovskite-based flexible photodetectors

In addition to the substrates, electrodes, and encapsulation layers, the flexibility of the perovskite films does have a distinct and decisive role in the performance of perovskite-based flexible devices. Despite the leaping advance in perovskite polycrystalline films-based devices, they suffer from high bulk defects, large grain boundaries, and serious performance loss due to the crack under operation (bending, folding, stretching, etc.) [125,126] or temperature change [127]. Low-dimensional perovskites possess the advantages of single-crystalline perovskites (low-density bulk defects and grain boundaries) and additionally salient mechanical flexibility, simultaneously [128]. Besides these, low-dimensional perovskites have also shown better stability than polycrystalline ones owing to their phase/environmental stability and suppressed ion migration. As shown in Fig. 15 [129–132], low-dimensional perovskites mainly consist of 0D particles (e.g., quantum dots and nanocrystals), 1D nanostructures (e.g., nanowires, nanotubes, nanorods), and 2D nanostructures (e.g., nanosheets, nanonets).

Typically, 0D perovskite quantum dots or nanocrystal films show the superior ability of light-harvesting than bulk counterparts, thus equipping 0D perovskite-based photodetectors a higher photocurrent, on/off ratio, and responsivity. For example, CsBr/KBr-mediated CsPbBr_3 quantum dots exhibited an improved surface morphology and crystallinity with reduced defect densities, obtaining a high responsivity of 10.1 A/W and an on/off ratio up to 10^4 . Moreover, the devices showed outstanding flexibility and electrical stability after 1600 bending cycles at an angle of 60° without degradation [133]. While, it is processed by spin-coating, suffering from a low materials utilization ratio below 1% and poor film quality in a large area. Spray-coated CsPbBr_3 quantum dot film-based photodiode also showed a low dark current density of 4×10^{-4} mA/cm² and a high responsivity of 3 A/W [27]. Besides quantum dots, perovskite nanoparticle-based flexible photodetectors were also constructed with the process presented in Fig. 15(a) [129]. The electrical performance of the flexible device maintained almost the same as that before bent, showing 0D perovskite a great potential in fabricating flexible devices. While the 0D perovskites suffer from poor interfacial carrier transport

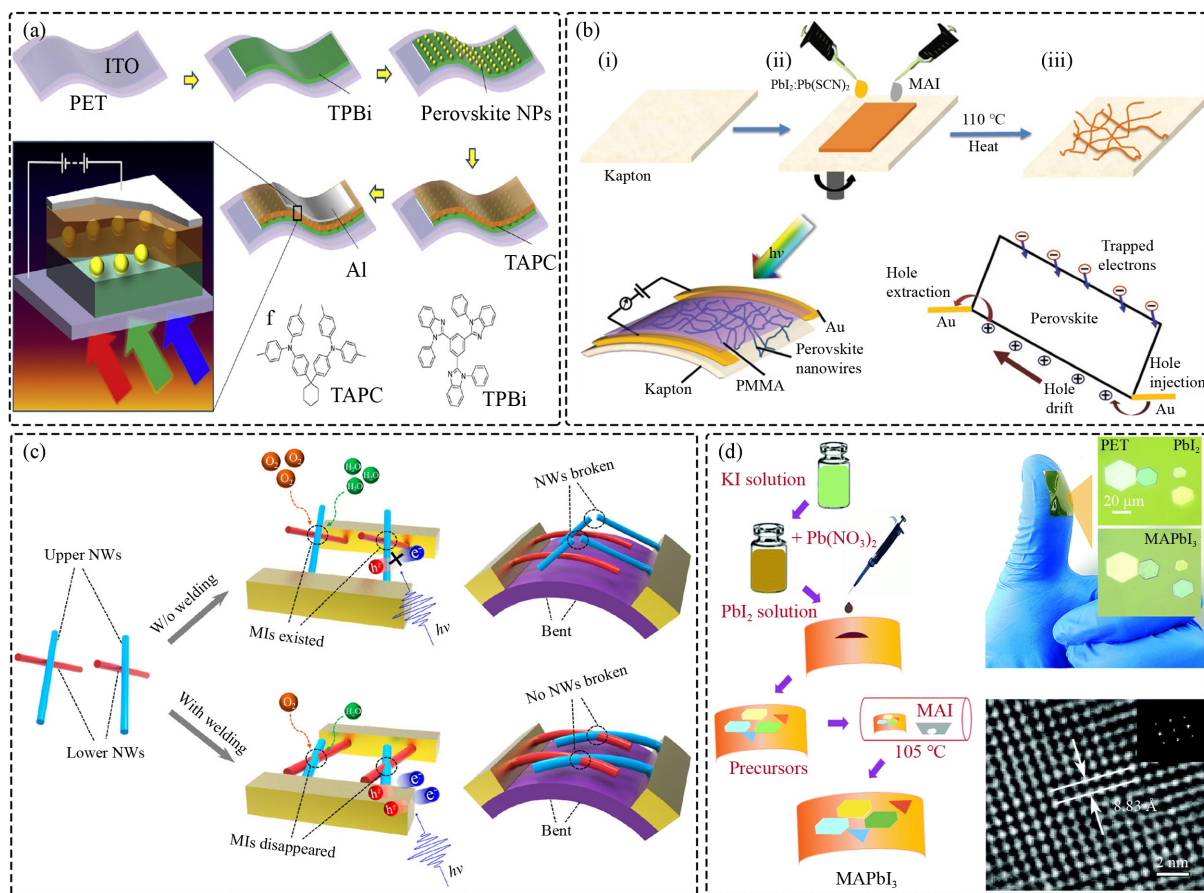


Fig. 15 Flexible photodetectors based on low-dimensional perovskites of (a) nanoparticles [129], (b,c) nanowires [130,131], and (d) nanoflakes [132]. Reprinted with permission from Ref. [129], copyright@2018, Elsevier. Reprinted with permission from Ref. [130], copyright@2019, Wiley-VCH. Reprinted with permission from Ref. [131], copyright@2020, American Chemical Society. Reprinted with permission from Ref. [132], copyright@2017, Royal Society of Chemistry.

and collection due to their isolated states. Integrating 0D perovskite quantum dots with carbon nanotubes has been demonstrated to be a powerful approach to improving performance [134,135].

Compared with 0D perovskites, 1D perovskites with well-defined structures provide more direct charge transport pathways, benefitting from low defect/trap densities and reduced carrier recombination. As shown in Fig. 15(b) [130], high-quality perovskite nanowires were grown on a Kapton substrate through an all-solution-based technique. The photodetector exhibited an ultrafast response speed with a rising time of 227.2 μ s. Moreover, highly stable perovskite nanowire-based flexible photodetectors have also been demonstrated without degradation under exposure for more than 5000 h [136] or ~10000 times bending [137]. However, the nanowires network contains many micro interfaces between nanowires, by which the carriers' transport was hindered and water-oxygen molecules were absorbed, seriously limiting the device's performance and stability. As depicted in Fig. 15(c) [131], a welding strategy was demonstrated to reduce the micro interfaces greatly, facilitating all the

nanowires to form a film without stacking. The welded devices possessed a better performance with ultrahigh stability.

2D layered perovskite films with atomic thickness are expected to have faster in-plane charge carrier transport owing to the absence of hopping barriers. As shown in Fig. 15(d) [132], highly crystalline perovskite nanoflakes were fabricated through a low-temperature solution-assisted vapour method, where one precursor of the perovskite spin-coated first and reacted with the vapour of the other precursor at a low temperature to synthesize perovskite nanoflakes. Compared with the traditional CVD methods, this method can be applied to any substrate without restriction, broadening the fabrication methods of 2D perovskite-based flexible devices.

4.5 Elaborate device structures for flexible photodetectors

As described above, flexible substrates, soft electrodes, conformal encapsulation, and low-dimensional perovskite can promote the flexibility of devices to a great extent. Besides these, designing elaborate device structures is

another route to collaborate with them. Figure 16 [138–141] concludes some novel device structures, of which the mechanisms for enhancing flexibility are tailoring the neutral plane of devices or releasing strains through the structures themselves.

As shown in Fig. 16(a) [138], the PS bead monolayer was formed by rubbing the powders unidirectionally through two layers of PDMS and adhering the PS to the PMMA layer then by pressing the upper PDMS. The flexible photodetectors with an assembled polymeric microbead monolayer on the top surface show significantly improved mechanical durability at a submillimeter bending radius. To explore the reasons for flexibility enhancement, the von Mises stress and the neutral plane of the control and PMMA/PS devices were demonstrated with unchanged values. While, the maximum value of the plastic stress of the PMMA/PS devices was reduced greatly, possibly benefitting from the adhesion of PMMA to the perovskite film. Since PMMA shows higher flexibility than that of the perovskite, making the strain released by the adhesion layer during mechanical bending, and benefitting quick recovery of flexible photodetector from deformation meanwhile. To simplify the processes, PS beads were added to the perovskite precursors solution directly, facilitating a PS-incorporated perovskite photodetector as

shown in Fig. 16(b) [139]. The mechanical stability was also enhanced owing to the porous device structure, which can endure repeated bending without failure.

Besides the above-mentioned structures, nature-inspired structures such as nacre-like “brick-and-mortar” structures and spine-inspired structures were also constructed, as presented in Figs. 16(c) [140] and 16(d) [141]. Inspired by nacres, a monolayer of silica (SiO_2) and PS spheres was assembled by unidirectionally rubbing, on which the perovskite precursors solution spin-coated. A PS-gulped perovskite heterojunction device was formatted, where the crystal grains of perovskite film were glued by the PS and its surface was capped by a thin PS polymer layer. The synergistic effect of the PS-glued heterostructure enhanced the device ductility, and the stress or strain was released by the deformable PS/perovskite porous structure, thus improving the mechanical robustness and endurance, greatly. Similarly, PEDOT:EVA (poly(3,4-ethylenedioxy-thiophene):poly(ethylene-co-vinyl acetate)) was added as a glued polymer between ITO and perovskite film, which can absorb and release the stress efficiently like the spinal cartilage. Besides, the mechanical force was distributed evenly without pressure reduction owing to the adhesiveness of the PEDOT:EVA layer.

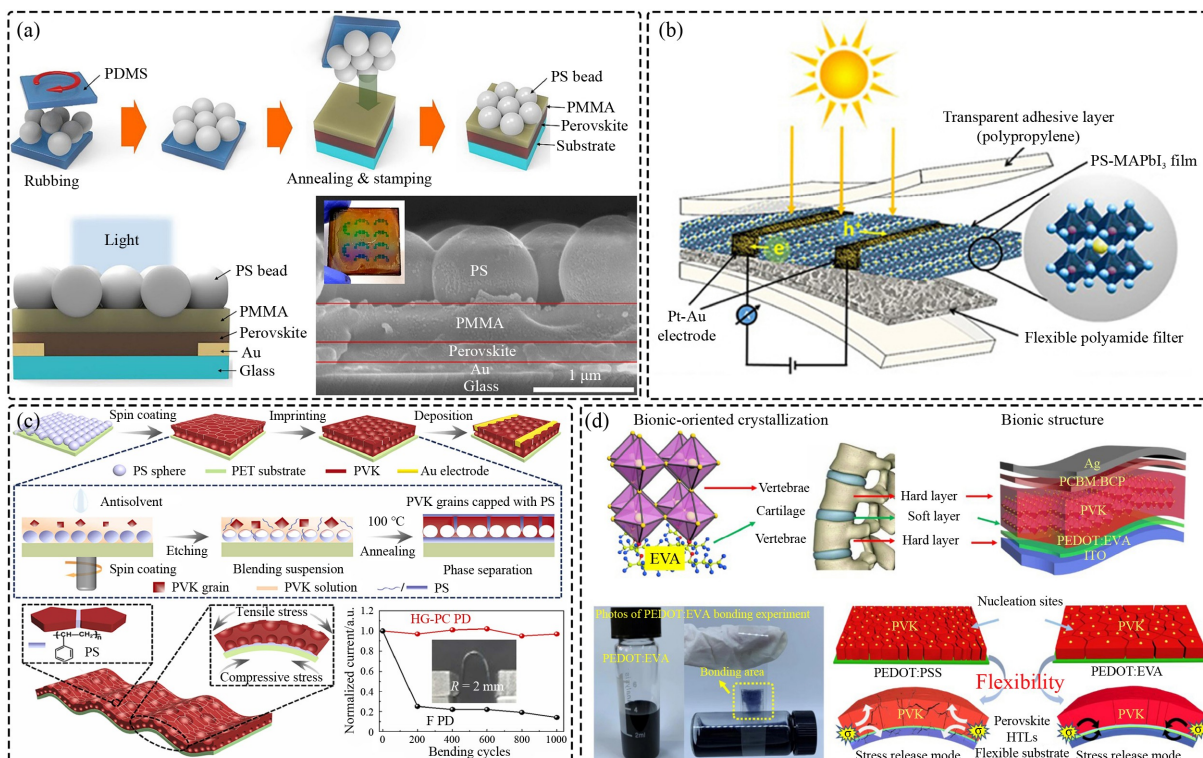


Fig. 16 Flexible photodetectors with (a) assembled polystyrene (PS) bead [138], (b) polymer composite [139], (c) nacre-inspired “brick-and-mortar” [140], and (d) vertebrate-like structures [141]. EVA: ethylene-vinyl acetate, PDMS: polydimethylsiloxane, PMMA: poly(methyl methacrylate). Reprinted with permission from Ref. [138], copyright@2021, Elsevier. Reprinted with permission from Ref. [139], copyright@2020, Springer Nature. Reprinted with permission from Ref. [140], copyright@2022, Elsevier. Reprinted with permission from Ref. [141], copyright@2020, Springer Nature.

5 Applications of flexible photodetectors

The era of flexible device approaches. Flexible photodetectors as significant components have witnessed a leap in development, with a conclusion shown in Table 3 [71,75,81,142–164]. As the table displays, the performance parameters of the perovskites-based photodetectors are superior to that of non-perovskite-based ones in responsivity, detectivity, LDR, and response time. Compared with the perovskites-based photodetectors on rigid, the performances of flexible ones don't lose to that of the rigid ones, even exceed them. Precisely because of their salient performance, flexible photodetectors have shown emerged in applications of various fields, such as the Internet of Things, intelligent sensors, and smart health. Among them, flexible photodetectors play roles in optical communication, imaging sensing, and health

monitoring, respectively. In this section, we will summarize the recent application development of perovskite-based flexible photodetectors.

5.1 Optical communication

During the last few years, mobile devices and wireless services have witnessed exponential growth, resulting in huge demand for radio frequency-based technologies [165]. As the imminent approximation of the next revolution in computing, the Internet of Things predicts that every device will have connectivity, requiring even more resources either from the devices themselves or the supporting network infrastructures [166]. As a consequence, the “Wi-Fi Spectrum Crunch” occurs [167]. Optical communication transmits information to the air atmosphere through lights, showing apparent advantages of low cost, rich spectra, less electromagnetic radiation,

Table 3 Performance comparison among non-perovskite-based flexible photodetectors, perovskite-based flexible ones, and perovskite-based rigid ones

Material	Device properties			Device performances				Ref.
	Substrate	Waveband	Structure	Responsivity/(A·W ⁻¹)	Detectivity/Jones	LDR/dB	Response time	
Sb ₂ Se ₃	Flexible	Infrared	Photoconductor	0.155	8.58×10^{10}	–	35/38 ms	[142]
MoS ₂	Flexible	Visible	Photoconductor	540	$\sim 1 \times 10^{12}$	–	0.5/1.15 s	[143]
InSe	Flexible	Visible	Photoconductor	56	1.92×10^{11}	–	~ 0.17 s	[144]
GaTe	Flexible	Visible	Photoconductor	240.3	–	–	0.4/0.5 s	[145]
ZnO	Flexible	Ultraviolet	Photoconductor	3.24	29.6	–	17.9/46.6 s	[146]
Ga ₂ O ₃	Flexible	Ultraviolet	Photovoltaic	22.75	8.2×10^{13}	97.6	–	[147]
MAPbI ₃	Rigid	Visible	Photoconductor	24.8	7.7×10^{12}	–	4/5.8 ms	[148]
MAPbI ₃	Flexible	Infrared	Photoconductor	0.036	–	–	< 0.1 s	[149]
MAPbI ₃	Rigid	Infrared	Photovoltaic	0.14	7.37×10^{11}	192	27 ns	[150]
MAPbI ₃	Flexible	Infrared	Photovoltaic	0.418	1.22×10^{13}	–	–	[151]
MAPbBr ₃	Rigid	Visible	Photoconductor	> 4000	$> 1 \times 10^{13}$	–	~ 25 μ s	[152]
MAPbBr ₃	Flexible	Visible	Photoconductor	5600	6.59×10^{11}	–	3.2/9.2 μ s	[75]
MAPbBr ₃	Rigid	Visible	Photovoltaic	0.26	1.5×10^{13}	256	100 ns	[71]
MAPbCl ₃	Rigid	Ultraviolet	Photoconductor	0.07	$> 1 \times 10^{11}$	–	43/37 ms	[153]
MAPbCl ₃	Rigid	Ultraviolet	Photovoltaic	> 0.15	$\sim 6 \times 10^{12}$	190	15 ns	[154]
MAPbCl ₃	Flexible	Ultraviolet	Photovoltaic	0.359	7.95×10^{12}	–	3.91/4.55 ms	[155]
CsPbBr ₃	Rigid	Visible	Photoconductor	55	9×10^{12}	–	0.43/0.31 ms	[156]
CsPbBr ₃	Flexible	Visible	Photoconductor	31.1	–	85	16 μ s	[81]
CsPbBr ₃	Rigid	Visible	Photovoltaic	~ 10	1.88×10^{13}	172.7	28/270 μ s	[157]
CsPbBr ₃	Flexible	Visible	Photovoltaic	10.1	9.35×10^{13}	–	–	[133]
CsPbCl ₃	Rigid	Ultraviolet	Photoconductor	2.11	5.6×10^{12}	57	77/63 ms	[158]
CsPbCl ₃	Flexible	Ultraviolet	Photoconductor	$> 1 \times 10^6$	2×10^{13}	–	0.3/0.35 s	[159]
CsPbCl ₃	Rigid	Ultraviolet	Photovoltaic	0.19	5.47×10^{12}	–	4.27/14.9 μ s	[160]
CsPbCl ₃	Flexible	Ultraviolet	Photovoltaic	0.12	1.4×10^{13}	136	~ 50 μ s	[161]
Cs ₂ AgBiBr ₆	Rigid	Ultraviolet	Photoconductor	7.01	5.66×10^{11}	–	956/995 μ s	[162]
Cs ₂ AgBiBr ₆	Rigid	Ultraviolet	Photovoltaic	0.075	1.87×10^{12}	100	0.24/0.29 ms	[163]
Cs ₂ AgBiBr ₆	Flexible	Ultraviolet	Photovoltaic	0.23	1.6×10^{13}	177.8	3.7/3.2 μ s	[164]

good confidentiality, and so on, which can potentially serve as a complementary technology to the current technologies [168].

Optical communication can be divided into visible and ultraviolet light communication according to the lights used in the system. A typical optical communication system and application are shown in Fig. 17 [169,170], which contains a light transmitter (LED), a light receiver (photodetectors), and periphery circuits. During communication, the data (audio or characters) was converted into a data stream first and transferred to the master controller by wired or wireless connection (Bluetooth, Wi-Fi, or Zigbee). Then, the state of the LED was manipulated by an ultrahigh-frequency according to the binary data, where LED off/on defines “0/1”. The photodetector responded to the emitting light from the LED directly, converting the light signal into binary data. A circle of optical communication was completed when the binary data was received by the point controller. Through high-frequency periodic repetition, data streams can be transported to the information processing unit and converted into text or video, as presented in Fig. 17(b) [170].

There are apparent restrictions in the applications of optical communication. For example, the quality of the light signal will incur loss due to particle diffusion and inherent interference of ambient light during the light transmission [171]. To diminish the signal attenuation and interference, three-electrode receivers and filters are necessary, which should be taken into consideration in the design of an optical communication system [172].

5.2 Image sensing

Image sensors, converting optical images into electrical signal “images” aided by the photoelectric effect of semiconductor materials have been widely utilized in

military reconnaissance, biological medicine, and digital photography [173]. Up to now, most commercial digital image sensors, like charge-coupled devices (CCDs) and complementary metal-oxide-semiconductor (CMOS) devices are usually based on amorphous or crystalline silicon (Si) [174]. Despite the mature technology and convenient operation, weak light absorption and poor mechanical flexibility make it difficult to be used in flexible image sensors [175], making thicker photoactive films usually needed. While, the device’s flexibility often negatively correlates with its thickness, thus resulting in a conflict between the device’s flexibility and performance. Recently, perovskite has attracted enormous attention for the preparation of high-performance flexible image sensors owing to its excellent optoelectronic properties and compatible process with flexible devices.

Perovskite-based image sensors are usually in the form of arrays, where an individual photodetector serves as a pixel. The optical image is captured by the photodetector array first and converted into corresponding data to trace the light intensity and color distribution in the two-dimensional space. To obtain a high-definition image, the density of the array needs to be high enough in a certain substrate area. For this purpose, the photolithography technique is always necessary [176,177], where the substrates are limited to be hard for the processes of evenly dividing glue and exposal operations in a plane surface. To combine the perovskite arrays with the photolithography technique, the process of fabricating a perovskite-based flexible image sensor is composed of constructing a perovskite-based photodetector array on the hard/flexible complex substrates and peeling off the flexible device from the hard substrates [110]. The complex substrates are often vertically stacked and bonded through the viscosity force of the flexible substrates. To make the peel-off process easy, a sacrificial layer (water-soluble or heat-resoluble) sandwiched by the

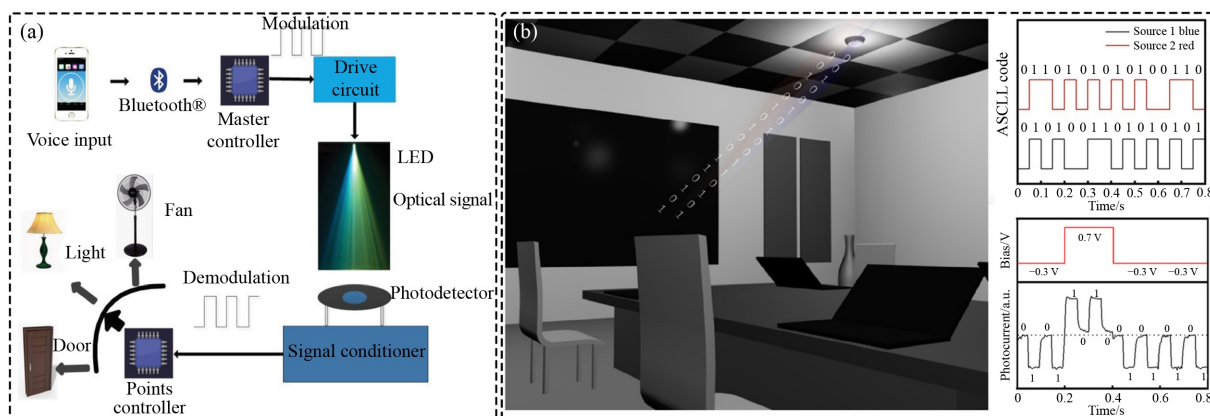


Fig. 17 (a) Schematic diagram [169] and (b) application demonstration of the optical communication system [170]. Reprinted with permission from Ref. [169], copyright@2020, Wiley-VCH. Reprinted with permission from Ref. [170], copyright@2020, American Chemical Society.

hard and flexible substrates is always needed. For the aspect of imaging application, typical function demonstrations are displayed in Fig. 18 [178–181]. As demonstrated in Figs. 18(a) [178] and 18(b) [179], perovskite-based flexible image sensors show the function of 2D code recognition and fingerprint identification.

On the other hand, flexible image sensors have the advantage of conforming themselves to curved surfaces, showing great potential in 3D imaging or curved imaging.

To fabricate flexible image sensors on curved surfaces, there are generally two strategies: fabricating flexible photodetector arrays on complex substrates, peeling off the flexible devices, and conforming the flexible ones to the curved target surfaces, or directly fabricating perovskite photodetector arrays on curved models through vacuum deposition methods. As presented in Fig. 18(c) [180], the photodetector arrays were fabricated on a polymer substrate and transferred onto various surfaces,

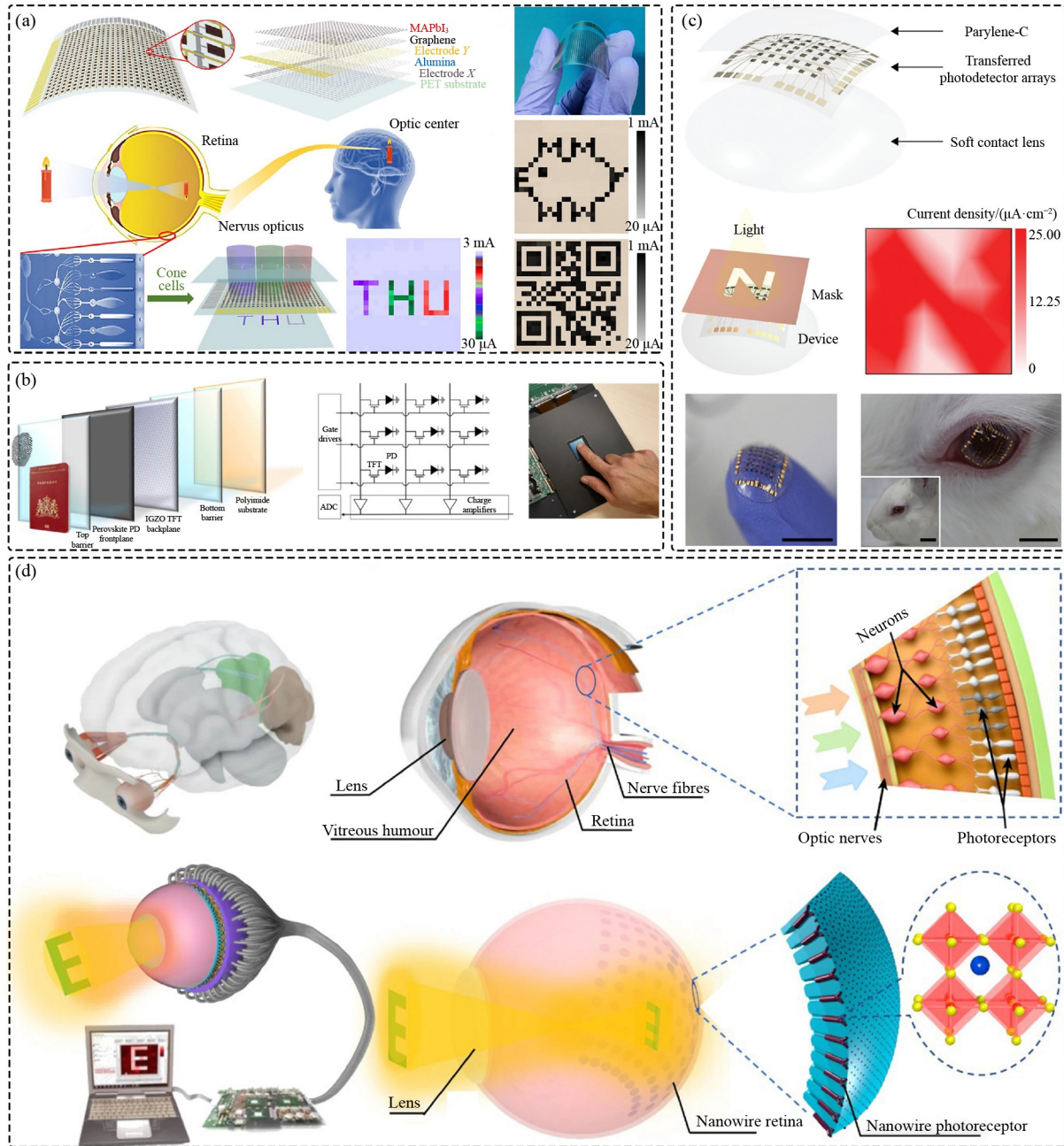


Fig. 18 Schematic diagrams of flexible photodetectors and their application demonstrations in (a) 2D code recognition [178], (b) fingerprint recognition [179], (c) 3D imaging [180], and (d) retina-like imaging [181]. Reprinted with permission from Ref. [178], copyright@2020, Elsevier. Reprinted with permission from Ref. [179], copyright@2021, Springer Nature. Reprinted with permission from Ref. [180], copyright@2021, Wiley-VCH. Reprinted with permission from Ref. [181], copyright@2020, Springer Nature.

design of flexible substrates (i.e., polymer, carbon cloth, fiber, paper, etc.), soft electrodes (i.e., metal-based conductive networks, carbon-based conductive materials, and 2D conductive materials, etc.), and conformal encapsulation (single-layer and multilayer stacked encapsulation) are presented. Low-dimensional perovskites (0D, 1D, and 2D nanostructures) and elaborate device structures are further introduced to enhance the flexibility of the perovskite-based flexible photodetectors. Typical applications of perovskite-based flexible photodetectors such as optical communication, image sensing, and health monitoring are also exhibited to learn the flexible photodetectors on a deeper level. The processing methods and applications demonstration of perovskite-based flexible photodetectors in this review would shed light on the design of devices and guide the direction of exploring their new applications in the industry, life, and health care.

Although perovskite-based flexible photodetectors have witnessed stirring achievements, they are still in their early stages of development. Practical applications of perovskite-based flexible photodetectors still face many intractable problems.

As for the perovskite materials alone, their instability is a major obstacle, which may degrade rapidly once explored in the moisture, thermal, and UV light for a long time. While these harsh conditions are always inevitable for outdoor applications. To make things worse, this degradation is irreversible, going against the long-term operation of the devices. Additive and component engineering can ameliorate the circumstance to some extent. Exploring effective encapsulation materials and strategies is a key approach to remitting this problem.

During processing, the operation stability of flexible devices is a significant factor, which includes not only the stability of the materials under harsh conditions but also the mechanical flexibility of devices under bending or stretching conditions. To enhance the mechanical flexibility of devices, each element of the devices needs to be mechanically flexible, including substrates, electrodes, perovskite, and encapsulation layers. The substrate materials employed now suffer from limited transparency, flexibility, or morphological plasticity. Thus, searching for new substrate materials to satisfy these requirements is necessary. Electrode materials with high conductivity, flexibility, and transparency can further shrink the thickness of the electrodes and broaden their application range of photodetectors. Encapsulation is the final procedure in the fabrication of perovskite-based flexible photodetectors, of which the materials and methods need to be considered carefully. The encapsulation materials need to prevent external moisture, oxygen, heat, and do not harm to under-layer perovskite films. Besides the encapsulation materials alone, the processes need also to do, since high temperature or usage of non-polar solvent would damage the perovskites.

It is not enough for the encapsulation layers to satisfy the above-mentioned conditions, the final thickness of the devices should also be controlled strictly, where most of the device thickness is shared by the substrate and encapsulation layers. Besides, cracks may also appear during long-term operation even, making performance degradation happen in advance. Therefore, an additional self-repairing capability seems to be particularly significant.

Applying the perovskite-based flexible photodetectors in practice implies both opportunities and challenges, for it requires the devices' performance to vary with scenarios, such as a high response speed in optical communication, a high signal contrast in image sensors, and a high responsivity in health monitoring. Many performance parameters of the perovskite-based flexible photodetectors fall behind the ones of the devices based on other semiconductors, let alone after long-term flexible operations. Thus, there is a long way from the laboratory to the applications for high-performance and stable perovskite-based flexible devices. Once it is achieved, wearable devices are bound to thrive, and the industry and human life will go through a new revolution, then.

Nomenclature

Abbreviations

ALD	Atomic layer deposition
CCD	Charge-coupled device
CMOS	Complementary metal-oxide-semiconductor
CVD	Chemical vapor deposition
DMF	N,N-dimethylformamide
DMSO	Dimethyl sulfide
e-h	Electron-hole
EQE	External quantum efficiency
EVA	Ethylene-vinyl acetate
FET	Field-effect transistor
FTO	Fluorine-doped tin oxide
ITO	Indium-tin-oxide
LDR	Linear dynamic range
LED	Light-emitting diode
NEP	Noise equivalent power
PDMS	Polydimethylsiloxane
PECVD	Plasma enhanced chemical vapor deposition
PEDOT:EVA	Poly(3,4-ethylenedioxy-thiophene):poly(ethylene-co-vinyl acetate)
PEN	Polyethylenenaphthalate
PET	Polyethylene terephthalate

PI	Polyimide
PLQY	Photoluminescence quantum yield
PMMA	Poly(methyl methacrylimide)
PPG	Photoplethysmography
PS	Polystyrene
PVDF	Polyvinylidene fluoride

Variables

h	Planck's constant
c	Speed of light
d	Channel length of photodetector
D^*	Specific detectivity
Δf	Bandwidth
G	Photoconductive gain
q	Elementary electron charge
I_{dark}	Dark current
I_{light}	Light current
P_{in}	Power density of incident light
P_{max}	Maximum detectable light density
P_{min}	Minimum detectable light density
R	Responsivity
S	Effective area of photodetector
V	Bias voltage
λ	Wavelength of light
τ_{fall}	Falling time
τ_{lifetime}	Carrier lifetime
τ_{rise}	Rising time
τ_{transit}	Carrier transit time
μ	Carrier mobility

Acknowledgements The authors acknowledge the financial support from the National Key R&D Program of China (Grant No. 2019YFB1503200), the National Natural Science Foundation of China (Grant Nos. 51905203 and 52275562), and the Fund from the Science, Technology, and Innovation Commission of Shenzhen Municipality, China (Grant No. JCYJ20190809100209531).

Conflict of Interest The authors declare that they have no conflict of interest.

Open Access This article is licensed under a Creative Commons Attribution 4.0 International License, which permits use, sharing, adaptation, distribution, and reproduction in any medium or format as long as appropriate credit is given to the original author(s) and source, a link to the Creative Commons license is provided, and the changes made are indicated.

The images or other third-party material in this article are included in the article's Creative Commons license, unless indicated otherwise in a credit line to the material. If material is not included in the article's Creative Commons license and your intended use is not permitted by statutory regulation or exceeds the permitted use, you will need to obtain permission directly from the copyright holder.

Visit <http://creativecommons.org/licenses/by/4.0/> to view a copy of this license.

References

1. He Z Q, Wang K, Zhao Z, Zhang T H, Li Y H, Wang L. A wearable flexible acceleration sensor for monitoring human motion. *Biosensors*, 2022, 12(8): 620
2. Wang Y, Sun L J, Wang C, Yang F X, Ren X C, Zhang X T, Dong H L, Hu W P. Organic crystalline materials in flexible electronics. *Chemical Society Reviews*, 2011, 40(1): 15–18
3. Chen X, Pan S, Feng P J, Bian H F, Han X, Liu J H, Guo X, Chen D Z, Ge H X, Shen Q D. Bioinspired ferroelectric polymer arrays as photodetectors with signal transmissible to neuron cells. *Advanced Materials*, 2016, 28(48): 10684–10691
4. Dong T, Simões J, Yang Z C. Flexible photodetector based on 2D materials: processing, architectures, and applications. *Advanced Materials Interfaces*, 2020, 7(4): 1901657
5. Xie C, Yan F. Flexible photodetectors based on novel functional materials. *Small*, 2017, 13(43): 1701822
6. Zhang Y Q. The application of third generation semiconductor in power industry. In: *Proceedings of the 10th Chinese Geosynthetics Conference & International Symposium on Civil Engineering and Geosynthetics (ISCEG 2020)*. Chengdu: E3S Web of Conferences, 2020, 198: 04011
7. Li J F, Li C F, Xu M S, Ji Z W, Shi K J, Xu X L, Li H B, Xu X G. “W-shaped” injection current dependence of electroluminescence line width in green InGaN/GaN-based LED grown on silicon substrate. *Optics Express*, 2017, 25(20): A871–A879
8. Zhu D L, Luo W B, Pan T S, Huang S T, Zhang K S, Xie Q, Shuai Y, Wu C G, Zhang W L. Fabrication of large-scale flexible silicon membrane by crystal-ion-slicing technique using BCB bonding layer. *Applied Physics A*, 2021, 127(9): 672
9. Chen X H, Yin L, Lv J, Gross A J, Le M, Gutierrez N G, Li Y, Jeerapan I, Giroud F, Berezovska A, O'Reilly R K, Xu S, Cosnier S, Wang J. Stretchable and flexible buckypaper-based lactate biofuel cell for wearable electronics. *Advanced Functional Materials*, 2019, 29(46): 1905785
10. Rajendran V, Mohan A M V, Jayaraman M, Nakagawa T. All-printed, interdigitated, freestanding serpentine interconnects based flexible solid state supercapacitor for self-powered wearable electronics. *Nano Energy*, 2019, 65: 104055
11. Yin L, Lv J, Wang J. Structural innovations in printed, flexible, and stretchable electronics. *Advanced Materials Technologies*, 2020, 5(11): 2000694
12. Xu Y L, Lin Q Q. Photodetectors based on solution-processable semiconductors: recent advances and perspectives. *Applied Physics Reviews*, 2020, 7(1): 011315
13. Liang J B, Takatsuki D, Higashiwaki M, Shimizu Y, Ohno Y, Nagai Y, Shigekawa N. Fabrication of β -Ga₂O₃/Si heterointerface and characterization of interfacial structures for high-power device applications. *Japanese Journal of Applied Physics*, 2022, 61(SF): SF1001
14. Dong H, Ran C X, Gao W Y, Li M J, Xia Y D, Huang W. Metal halide perovskite for next-generation optoelectronics: progresses and prospects. *eLight*, 2023, 3(1): 3

15. Kim W, Kim H, Yoo T J, Lee J Y, Jo J Y, Lee B H, Sasikala A A, Jung G Y, Pak Y. Perovskite multifunctional logic gates via bipolar photoresponse of single photodetector. *Nature Communications*, 2022, 13(1): 720
16. Roy P, Ghosh A, Barclay F, Khare A, Cuce E. Perovskite solar cells: a review of the recent advances. *Coatings*, 2022, 12(8): 1089
17. He C L, Liu X G. The rise of halide perovskite semiconductors. *Light: Science & Applications*, 2023, 12(1): 15
18. Dey A, Ye J Z, De A, Debroye E, Ha S K, Bladt E, Kshirsagar A S, Wang Z Y, Yin J, Wang Y, Quan L N, Yan F, Gao M Y, Li X M, Shamsi J, Debnath T, Cao M H, Scheel M A, Kumar S, Steele J A, Gerhard M, Chouhan L, Xu K, Wu X G, Li Y X, Zhang Y N, Dutta A, Han C, Vincon I, Rogach A L, Nag A, Samanta A, Korgel B A, Shih C J, Gamelin D R, Son D H, Zeng H B, Zhong H Z, Sun H D, Demir H V, Scheblykin I G, Mora-Seró I, Stolarczyk J K, Zhang J Z, Feldmann J, Hofkens J, Luther J M, Pérez-Prieto J, Li L, Manna L, Bodnarchuk M I, Kovalenko M V, Roeffaers M B J, Pradhan N, Mohammed O F, Bakr O M, Yang P D, Müller-Buschbaum P, Kamat P V, Bao Q L, Zhang Q, Krahne R, Galian R E, Stranks S D, Bals S, Biju V, Tisdale W A, Yan Y, Hoye R L Z, Polavarapu L. State of the art and prospects for halide perovskite nanocrystals. *ACS Nano*, 2021, 15(7): 10775–10981
19. Ye J Z, Byrnavand M M, Martínez C O, Hoye R L Z, Saliba M, Polavarapu L. Defect passivation in lead-halide perovskite nanocrystals and thin films: toward efficient LEDs and solar cells. *Angewandte Chemie*, 2021, 133(40): 21804–21828
20. Koren E, Lörtscher E, Rawlings C, Knoll A W, Duerig U. Adhesion and friction in mesoscopic graphite contacts. *Science*, 2015, 348(6235): 679–683
21. Liu Y C, Yang Z, Liu S Z. Recent progress in single-crystalline perovskite research including crystal preparation, property evaluation, and applications. *Advanced Science*, 2018, 5(1): 1700471
22. Ng C H, Nishimura K, Ito N, Hamada K, Hirotani D, Wang Z, Yang F, Likubo S, Shen Q, Yoshino K, Minemoto T, Hayase S. Role of GeI_2 and SnF_2 additives for SnGe perovskite solar cells. *Nano Energy*, 2019, 58: 130–137
23. Brosch M, Deckert M, Rath S, Takagaki K, Weidner T, Ohl F W, Schmidt B, Lippert M T. An optically transparent multi-electrode array for combined electrophysiology and optophysiology at the mesoscopic scale. *Journal of Neural Engineering*, 2020, 17(4): 046014
24. Lee S M, Cho Y, Kim D Y, Chae J S, Choi K C. Enhanced light extraction from mechanically flexible, nanostructured organic light-emitting diodes with plasmonic nanomesh electrodes. *Advanced Optical Materials*, 2015, 3(9): 1240–1247
25. Wu C Y, Wang Z Y, Liang L, Gui T J, Zhong W, Du R C, Xie C, Wang L, Luo L B. Graphene-assisted growth of patterned perovskite films for sensitive light detector and optical image sensor application. *Small*, 2019, 15(19): 1900730
26. Chaudhary S, Gupta S K, Singh Negi C M. Enhanced performance of perovskite photodetectors fabricated by two-step spin coating approach. *Materials Science in Semiconductor Processing*, 2020, 109: 104916
27. Yang Z, Wang M Q, Li J J, Dou J J, Qiu H W, Shao J Y. Spray-coated CsPbBr_3 quantum dot films for perovskite photodiodes. *ACS Applied Materials & Interfaces*, 2018, 10(31): 26387–26395
28. Tong S C, Gong C D, Zhang C J, Liu G, Zhang D, Zhou C H, Sun J, Xiao S, He J, Gao Y L, Yang J L. Fully-printed, flexible cesium-doped triple cation perovskite photodetector. *Applied Materials Today*, 2019, 15: 389–397
29. Tong S C, Wu H, Zhang C J, Li S G, Wang C H, Shen J Q, Xiao S, He J, Yang J L, Sun J, Gao Y L. Large-area and high-performance $\text{CH}_3\text{NH}_3\text{PbI}_3$ perovskite photodetectors fabricated via doctor blading in ambient condition. *Organic Electronics*, 2017, 49: 347–354
30. Wang Q L, Zhang G N, Zhang H Y, Duan Y Q, Yin Z P, Huang Y A. High-resolution, flexible, and full-color perovskite image photodetector via electrohydrodynamic printing of ionic-liquid-based ink. *Advanced Functional Materials*, 2021, 31(28): 2100857
31. Wei H M, Ma H, Tai M Q, Wei Y, Li D Q, Zhao X Y, Lin H, Fan S S, Jiang K L. Perovskite photodetectors prepared by flash evaporation printing. *RSC Advances*, 2017, 7(55): 34795–34800
32. Li W, Xu Y L, Peng J L, Li R M, Song J N, Huang H H, Cui L H, Lin Q Q. Evaporated perovskite thick junctions for X-ray detection. *ACS Applied Materials & Interfaces*, 2021, 13(2): 2971–2978
33. Zhang X N, Liu X Y, Sun B, Ye H B, He C H, Kong L X, Li G L, Liu Z Y, Liao G L. Ultrafast, self-powered, and charge-transport-layer-free ultraviolet photodetectors based on sequentially vacuum-evaporated lead-free $\text{Cs}_2\text{AgBiBr}_6$ thin films. *ACS Applied Materials & Interfaces*, 2021, 13(30): 35949–35960
34. Liu X Y, Liu Z Y, Li J J, Tan X H, Sun B, Fang H, Xi S, Shi T L, Tang Z R, Liao G L. Ultrafast, self-powered and charge-transport-layer-free photodetectors based on high-quality evaporated CsPbBr_3 perovskites for applications in optical communication. *Journal of Materials Chemistry C*, 2020, 8(10): 3337–3350
35. Tian C C, Wang F, Wang Y P, Yang Z, Chen X J, Mei J J, Liu H Z, Zhao D X. Chemical vapor deposition method grown all-inorganic perovskite microcrystals for self-powered photodetectors. *ACS Applied Materials & Interfaces*, 2019, 11(17): 15804–15812
36. Swartwout R, Hoerantner M T, Bulović V. Scalable deposition methods for large-area production of perovskite thin films. *Energy & Environmental Materials*, 2019, 2(2): 119–145
37. Dai X F, Xu K, Wei F A. Recent progress in perovskite solar cells: the perovskite layer. *Beilstein Journal of Nanotechnology*, 2020, 11: 51–60
38. Huang D W, Xie P F, Pan Z X, Rao H S, Zhong X H. One-step solution deposition of CsPbBr_3 based on precursor engineering for efficient all-inorganic perovskite solar cells. *Journal of Materials Chemistry A*, 2019, 7(39): 22420–22428
39. Wan X J, Yu Z, Tian W M, Huang F Z, Jin S Y, Yang X C, Cheng Y B, Hagfeldt A, Sun L C. Efficient and stable planar all-inorganic perovskite solar cells based on high-quality CsPbBr_3 films with controllable morphology. *Journal of Energy Chemistry*, 2020, 46: 8–15
40. Gong O Y, Seo M K, Choi J H, Kim S Y, Kim D H, Cho I S, Park

- N G, Han G S, Jung H S. High-performing laminated perovskite solar cells by surface engineering of perovskite films. *Applied Surface Science*, 2022, 591: 153148
41. Das S, Yang B, Gu G, Joshi P C, Ivanov I N, Rouleau C M, Aytug T, Geohegan D B, Xiao K. High-performance flexible perovskite solar cells by using a combination of ultrasonic spray-coating and low thermal budget photonic curing. *ACS Photonics*, 2015, 2(6): 680–686
 42. Kim H S, Im S H, Park N G. Organolead halide perovskite: new horizons in solar cell research. *The Journal of Physical Chemistry C*, 2014, 118(11): 5615–5625
 43. Ding X Y, Liu J H, Harris T A L. A review of the operating limits in slot die coating processes. *AIChE Journal*, 2016, 62(7): 2508–2524
 44. Huang K Q, Li H Y, Zhang C J, Gao Y X, Liu T J, Zhang J, Gao Y L, Peng Y Y, Ding L M, Yang J L. Highly efficient perovskite solar cells processed under ambient conditions using *in situ* substrate-heating-assisted deposition. *Solar RRL*, 2019, 3(3): 1800318
 45. Liu B T, Yang J H, Huang Y S. Highly efficient perovskite solar cells fabricated under a 70% relative humidity atmosphere. *Journal of Power Sources*, 2021, 500: 229985
 46. Dehghani A, Jahanshah F, Borman D, Dennis K, Wang J. Design and engineering challenges for digital ink-jet printing on textiles. *International Journal of Clothing Science and Technology*, 2004, 16(1/2): 262–273
 47. Khan A, Rahman K, Kim D S, Choi K H. Direct printing of copper conductive micro-tracks by multi-nozzle electrohydrodynamic inkjet printing process. *Journal of Materials Processing Technology*, 2012, 212(3): 700–706
 48. Li Y C, Shi B, Xu Q J, Yan L L, Ren N Y, Chen Y L, Han W, Huang Q, Zhao Y, Zhang X D. Wide bandgap interface layer induced stabilized perovskite/silicon tandem solar cells with stability over ten thousand hours. *Advanced Energy Materials*, 2021, 11(48): 2102046
 49. Zhang Y L, Huang Y, Zhou C W, Xu Y F, Zhong J Q, Mao H Y. Crystalline structures and optoelectronic properties of orthorhombic CsPbBr₃ polycrystalline films grown by the co-evaporation method. *Vacuum*, 2022, 202: 111219
 50. Li C W, Song Z N, Chen C, Xiao C X, Subedi B, Harvey S P, Shrestha N, Subedi K K, Chen L, Liu D C, Li Y, Kim Y W, Jiang C S, Heben M J, Zhao D W, Ellingson R J, Podraza N J, Al-Jassim M, Yan Y F. Low-bandgap mixed tin-lead iodide perovskites with reduced methylammonium for simultaneous enhancement of solar cell efficiency and stability. *Nature Energy*, 2020, 5(10): 768–776
 51. Liang G X, Lan H B, Fan P, Lan C F, Zheng Z H, Peng H X, Luo J T. Highly uniform large-area (100 cm²) perovskite CH₃NH₃PbI₃ thin-films prepared by single-source thermal evaporation. *Coatings*, 2018, 8(8): 256
 52. Ahmadi M, Wu T, Hu B. A review on organic-inorganic halide perovskite photodetectors: device engineering and fundamental physics. *Advanced Materials*, 2017, 29(41): 1605242
 53. Chen H, Wang H, Wu J, Wang F, Zhang T, Wang Y F, Liu D T, Li S B, Penty R V, White I H. Flexible optoelectronic devices based on metal halide perovskites. *Nano Research*, 2020, 13(8): 1997–2018
 54. Wang Y, Li D L, Chao L F, Niu T T, Chen Y H, Huang W. Perovskite photodetectors for flexible electronics: recent advances and perspectives. *Applied Materials Today*, 2022, 28: 101509
 55. Hao D D, Zou J, Huang J. Recent developments in flexible photodetectors based on metal halide perovskite. *InfoMat*, 2020, 2(1): 139–169
 56. Li C L, Li J, Li Z P, Zhang H Y, Dang Y Y, Kong F G. High-performance photodetectors based on nanostructured perovskites. *Nanomaterials*, 2021, 11(4): 1038
 57. Wang Y, Zhang X W, Jiang Q, Liu H, Wang D G, Meng J H, You J B, Yin Z G. Interface engineering of high-performance perovskite photodetectors based on PVP/SnO₂ electron transport layer. *ACS Applied Materials & Interfaces*, 2018, 10(7): 6505–6512
 58. Tian W, Zhou H P, Li L. Hybrid organic-inorganic perovskite photodetectors. *Small*, 2017, 13(41): 1702107
 59. Miao J L, Zhang F J. Recent progress on highly sensitive perovskite photodetectors. *Journal of Materials Chemistry C*, 2019, 7(7): 1741–1791
 60. Yang Z, Dou J J, Wang M Q, Li J J, Huang J, Shao J Y. Flexible all-inorganic photoconductor detectors based on perovskite/hole-conducting layer heterostructures. *Journal of Materials Chemistry C*, 2018, 6(25): 6739–6746
 61. Li C L, Ma Y, Xiao Y F, Shen L, Ding L M. Advances in perovskite photodetectors. *InfoMat*, 2020, 2(6): 1247–1256
 62. Li L D, Ye S, Qu J L, Zhou F F, Song J, Shen G Z. Recent advances in perovskite photodetectors for image sensing. *Small*, 2021, 17(18): 2005606
 63. Li F, Ma C, Wang H, Hu W J, Yu W L, Sheikh A D, Wu T. Ambipolar solution-processed hybrid perovskite phototransistors. *Nature Communications*, 2015, 6(1): 8238
 64. García de Arquer F P, Armin A, Meredith P, Sargent E H. Solution-processed semiconductors for next-generation photodetectors. *Nature Reviews Materials*, 2017, 2(3): 16100
 65. Huang J F, Lee J, Nakayama H, Schrock M, Cao D X, Cho K, Bazan G C, Nguyen T Q. Understanding and countering illumination-sensitive dark current: toward organic photodetectors with reliable high detectivity. *ACS Nano*, 2021, 15(1): 1753–1763
 66. Kim H, Kang J, Ahn H, Jung I H. Contribution of dark current density to the photodetecting properties of thieno[3,4-b]pyrazine-based low bandgap polymers. *Dyes and Pigments*, 2022, 197: 109910
 67. De Fazio D, Uzlu B, Torre I, Monasterio-Balcells C, Gupta S, Khodkov T, Bi Y, Wang Z X, Otto M, Lemme M C, Goossens S, Neumaier D, Koppens F H L. Graphene-quantum dot hybrid photodetectors with low dark-current readout. *ACS Nano*, 2020, 14(9): 11897–11905
 68. Grimoldi A, Colella L, La Monaca L, Azzellino G, Caironi M, Bertarelli C, Natali D, Sampietro M. Inkjet printed polymeric electron blocking and surface energy modifying layer for low dark current organic photodetectors. *Organic Electronics*, 2016, 36: 29–34
 69. Zhao D P, Saputra R M, Song P, Yang Y H, Li Y Z. How

- graphene strengthened molecular photoelectric performance of solar cells: a photo current-voltage assessment. *Solar Energy*, 2021, 213: 271–283
70. Hu W H, Vael C, Diethelm M, Strassel K, Anantharaman S B, Aribia A, Cremona M, Jenatsch S, Nüesch F, Hany R. On the response speed of narrowband organic optical upconversion devices. *Advanced Optical Materials*, 2022, 10(17): 2200695
 71. Bao C X, Chen Z L, Fang Y J, Wei H T, Deng Y H, Xiao X, Li L L, Huang J S. Low-noise and large-linear-dynamic-range photodetectors based on hybrid-perovskite thin-single-crystals. *Advanced Materials*, 2017, 29(39): 1703209
 72. De Sanctis A, Jones G F, Wehenkel D J, Bezares F, Koppens F H L, Craciun M F, Russo S. Extraordinary linear dynamic range in laser-defined functionalized graphene photodetectors. *Science Advances*, 2017, 3(5): e1602617
 73. Zhang J, Li J A, Cheng W, Zhang J H, Zhou Z, Sun X D, Li L L, Liang J G, Shi Y, Pan L J. Challenges in materials and devices of electronic skin. *ACS Materials Letters*, 2022, 4(4): 577–599
 74. Han S T, Peng H Y, Sun Q J, Venkatesh S, Chung K S, Lau S C, Zhou Y, Roy V A L. An overview of the development of flexible sensors. *Advanced Materials*, 2017, 29(33): 1700375
 75. Jing H, Peng R W, Ma R M, He J, Zhou Y, Yang Z Q, Li C Y, Liu Y, Guo X J, Zhu Y Y, Wang D, Su J, Sun C, Bao W Z, Wang M. Flexible ultrathin single-crystalline perovskite photodetector. *Nano Letters*, 2020, 20(10): 7144–7151
 76. Lee Y H, Song I, Kim S H, Park J H, Park S O, Lee J H, Won Y, Cho K, Kwak S K, Oh J H. Perovskite granular wire photodetectors with ultrahigh photodetectivity. *Advanced Materials*, 2020, 32(32): 2002357
 77. Tan Q S, Ye G, Zhang Y, Du X J, Liu H N, Xie L M, Zhou Y, Liu N. Vacuum-filtration enabled large-area CsPbBr₃ films on porous substrates for flexible photodetectors. *Journal of Materials Chemistry C*, 2019, 7(43): 13402–13409
 78. Kim T, Jeong S, Kim K H, Shim H, Kim D, Kim H J. Engineered surface halide defects by two-dimensional perovskite passivation for deformable intelligent photodetectors. *ACS Applied Materials & Interfaces*, 2022, 14(22): 26004–26013
 79. Chen Y T, Zhao C Y, Zhang T T, Wu X H, Zhang W J, Ding S J. Flexible and filter-free color-imaging sensors with multicomponent perovskites deposited using enhanced vapor technology. *Small*, 2021, 17(26): 2007543
 80. Lédée F, Ciavatti A, Verdi M, Basiricò L, Fraboni B. Ultra-stable and robust response to X-rays in 2D layered perovskite micro-crystalline films directly deposited on flexible substrate. *Advanced Optical Materials*, 2022, 10(1): 2101145
 81. Li X M, Yu D J, Chen J, Wang Y, Cao F, Wei Y, Wu Y, Wang L, Zhu Y, Sun Z G, Ji J P, Shen Y L, Sun H D, Zeng H B. Constructing fast carrier tracks into flexible perovskite photodetectors to greatly improve responsivity. *ACS Nano*, 2017, 11(2): 2015–2023
 82. Liu S T, Liu X H, Zhu Z F, Wang S L, Gu Y, Shan F K, Zou Y S. Improved flexible ZnO/CsPbBr₃/Graphene UV photodetectors with interface optimization by solution process. *Materials Research Bulletin*, 2020, 130: 110956
 83. Wang Y, Liu W W, Xin W, Zou T T, Zheng X, Li Y S, Xie X H, Sun X J, Yu W L, Liu Z B, Chen S Q, Yang J J, Guo C L. Back-reflected performance-enhanced flexible perovskite photodetectors through substrate texturing with femtosecond laser. *ACS Applied Materials & Interfaces*, 2020, 12(23): 26614–26623
 84. Lei J, Gao F, Wang H X, Li J, Jiang J X, Wu X, Gao R R, Yang Z, Liu S Z. Efficient planar CsPbBr₃ perovskite solar cells by dual-source vacuum evaporation. *Solar Energy Materials and Solar Cells*, 2018, 187: 1–8
 85. Sun H X, Lei T Y, Tian W, Cao F R, Xiong J, Li L. Self-powered, flexible, and solution-processable perovskite photodetector based on low-cost carbon cloth. *Small*, 2017, 13(28): 1701042
 86. Ding D, Li H N, Yao H Z, Liu L, Tian B B, Su C L, Wang Y, Shi Y M. Template growth of perovskites on yarn fibers induced by capillarity for flexible photoelectric applications. *Journal of Materials Chemistry C*, 2019, 7(31): 9496–9503
 87. Sun H X, Tian W, Cao F R, Xiong J, Li L. Ultrahigh-performance self-powered flexible double-twisted fibrous broadband perovskite photodetector. *Advanced Materials*, 2018, 30(21): 1706986
 88. Kim H J, Oh H, Kim T, Kim D, Park M. Stretchable photodetectors based on electrospun polymer/perovskite composite nanofibers. *ACS Applied Nano Materials*, 2022, 5(1): 1308–1316
 89. Zheng Q H, Li H X, Zheng Y L, Li Y N, Liu X, Nie S X, Ouyang X H, Chen L H, Ni Y H. Cellulose-based flexible organic light-emitting diodes with enhanced stability and external quantum efficiency. *Journal of Materials Chemistry C*, 2021, 9(13): 4496–4504
 90. Hassan M, Abbas G, Li N, Afzal A, Haider Z, Ahmed S, Xu X R, Pan C F, Peng Z C. Significance of flexible substrates for wearable and implantable devices: recent advances and perspectives. *Advanced Materials Technologies*, 2022, 7(3): 2100773
 91. Zhang X Z, He D, Yang Q, Atashbar M Z. Rapid, highly sensitive, and highly repeatable printed porous paper humidity sensor. *Chemical Engineering Journal*, 2022, 433: 133751
 92. Li S X, Xu X L, Yang Y, Xu Y S, Xu Y, Xia H. Highly deformable high-performance paper-based perovskite photodetector with improved stability. *ACS Applied Materials & Interfaces*, 2021, 13(27): 31919–31927
 93. Wang W L, Li G L, Jiang Z H, Zhang Y, Hu T J, Yi J, Chu Z Y. Structural, optical and flexible properties of CH₃NH₃PbI₃ perovskite films deposited on paper substrates. *Optical Materials*, 2021, 114: 110926
 94. Fang H J, Li J W, Ding J, Sun Y, Li Q, Sun J L, Wang L D, Yan Q F. An origami perovskite photodetector with spatial recognition ability. *ACS Applied Materials & Interfaces*, 2017, 9(12): 10921–10928
 95. Yang Y, Hu H J, Chen Z Y, Wang Z Y, Jiang L M, Lu G X, Li X J, Chen R M, Jin J, Kang H C, Chen H X, Lin S, Xiao S Q, Zhao H Y, Xiong R, Shi J, Zhou Q F, Xu S, Chen Y. Stretchable nanolayered thermoelectric energy harvester on complex and dynamic surfaces. *Nano Letters*, 2020, 20(6): 4445–4453
 96. Chen X J, Gao X X, Nomoto A, Shi K, Lin M Y, Hu H J, Gu Y, Zhu Y Z, Wu Z H, Chen X, Wang X Y, Qi B Y, Zhou S, Ding H,

- Xu S. Fabric-substrated capacitive biopotential sensors enhanced by dielectric nanoparticles. *Nano Research*, 2021, 14(9): 3248–3252
97. Mathur A, Fan H, Maheshwari V. Soft polymer-organolead halide perovskite films for highly stretchable and durable photodetectors with Pt-Au nanochain-based electrodes. *ACS Applied Materials & Interfaces*, 2021, 13(49): 58956–58965
 98. Bao C X, Zhu W D, Yang J, Li F M, Gu S, Wang Y R Q, Yu T, Zhu J, Zhou Y, Zou Z G. Highly flexible self-powered organolead trihalide perovskite photodetectors with gold nanowire networks as transparent electrodes. *ACS Applied Materials & Interfaces*, 2016, 8(36): 23868–23875
 99. Yang J, Bao C X, Zhu K, Yu T, Xu Q Y. High-performance transparent conducting metal network electrodes for perovskite photodetectors. *ACS Applied Materials & Interfaces*, 2018, 10(2): 1996–2003
 100. Lin G M, Lin Y W, Sun B Y. Transparent graphene electrodes based hybrid perovskites photodetectors with broad spectral response from UV-visible to near-infrared. *Nanotechnology*, 2022, 33(8): 085204
 101. Kim J M, Kim S, Choi S H. High-performance n-i-p-type perovskite photodetectors employing graphene-transparent conductive electrodes n-type doped with amine group molecules. *ACS Sustainable Chemistry & Engineering*, 2019, 7(1): 734–739
 102. Jang W, Kim B G, Seo S, Shawky A, Kim M S, Kim K, Mikladal B, Kauppinen E I, Maruyama S, Jeon I, Wang D H. Strong dark current suppression in flexible organic photodetectors by carbon nanotube transparent electrodes. *Nano Today*, 2021, 37: 101081
 103. Marunchenko A A, Baranov M A, Ushakova E V, Ryabov D R, Pushkarev A P, Gets D S, Nasibulin A G, Makarov S V. Single-walled carbon nanotube thin film for flexible and highly responsive perovskite photodetector. *Advanced Functional Materials*, 2022, 32(12): 2109834
 104. Deng W, Huang H C, Jin H M, Li W, Chu X, Xiong D, Yan W, Chun F J, Xie M L, Luo C, Jin L, Liu C Q, Zhang H T, Deng W L, Yang W Q. All-sprayed-processable, large-area, and flexible perovskite/MXene-based photodetector arrays for photocommunication. *Advanced Optical Materials*, 2019, 7(6): 1801521
 105. Ren A B, Zou J H, Lai H G, Huang Y X, Yuan L M, Xu H, Shen K, Wang H, Wei S Y, Wang Y F, Hao X, Zhang J Q, Zhao D W, Wu J, Wang Z M. Direct laser-patterned MXene-perovskite image sensor arrays for visible-near infrared photodetection. *Materials Horizons*, 2020, 7(7): 1901–1911
 106. Hu J, Xiong X, Guan W, Xiao Z, Tan C, Long H. Durability engineering in all-inorganic CsPbX₃ perovskite solar cells: strategies and challenges. *Materials Today Chemistry*, 2022, 24: 100792
 107. Wu G B, Liang R, Ge M Z, Sun G X, Zhang Y, Xing G C. Surface passivation using 2D perovskites toward efficient and stable perovskite solar cells. *Advanced Materials*, 2022, 34(8): 2105635
 108. Cao Q, Wang T, Yang J B, Zhang Y X, Li Y K, Pu X Y, Zhao J S, Chen H, Li X Q, Tojiboyev I, Chen J Z, Etgar L, Li X H. Environmental-friendly polymer for efficient and stable inverted perovskite solar cells with mitigating lead leakage. *Advanced Functional Materials*, 2022, 32(32): 2201036
 109. Wu W Q, Wang X D, Han X, Yang Z, Gao G Y, Zhang Y F, Hu J F, Tan Y W, Pan A L, Pan C F. Flexible photodetector arrays based on patterned CH₃NH₃PbI_{3-x}Cl_x perovskite film for real-time photosensing and imaging. *Advanced Materials*, 2019, 31(3): 1805913
 110. Wu W Q, Han X, Li J, Wang X D, Zhang Y F, Huo Z H, Chen Q S, Sun X D, Xu Z S, Tan Y W, Pan C F, Pan A L. Ultrathin and conformable lead halide perovskite photodetector arrays for potential application in retina-like vision sensing. *Advanced Materials*, 2021, 33(9): 2006006
 111. Zhao F Y, Luo X, Gu C J, Chen J M, Hu Z Y, Peng Y Q. Novel 3D printing encapsulation strategies for perovskite photodetectors. *Advanced Materials Technologies*, 2022, 7(12): 2200521
 112. Ma S, Yuan G Z, Zhang Y, Yang N, Li Y J, Chen Q. Development of encapsulation strategies towards the commercialization of perovskite solar cells. *Energy & Environmental Science*, 2022, 15(1): 13–55
 113. Otero-Martínez C, Fiuza-Maneiro N, Polavarapu L. Enhancing the intrinsic and extrinsic stability of halide perovskite nanocrystals for efficient and durable optoelectronics. *ACS Applied Materials & Interfaces*, 2022, 14(30): 34291–34302
 114. Qaid S M H, Ghaithan H M, AlHarbi K K, Al-Asbahi B A, Aldwayyan A S. Enhancement of light amplification of CsPbBr₃ perovskite quantum dot films via surface encapsulation by PMMA polymer. *Polymers*, 2021, 13(15): 2574
 115. You X, Wu J J, Chi Y W. Superhydrophobic silica aerogels encapsulated fluorescent perovskite quantum dots for reversible sensing of SO₂ in a 3D-printed gas cell. *Analytical Chemistry*, 2019, 91(8): 5058–5066
 116. Xia B Z, Tu M, Pradhan B, Ceyssens F, Tietze M L, Rubio-Giménez V, Wauteraerts N, Gao Y J, Kraft M, Steele J A, Debroye E, Hofkens J, Ameloot R. Flexible metal halide perovskite photodetector arrays via photolithography and dry lift-off patterning. *Advanced Engineering Materials*, 2022, 24(1): 2100930
 117. Bose R, Yin J, Zheng Y Z, Yang C, Gartstein Y N, Bakr O M, Malko A V, Mohammed O F. Gentle materials need gentle fabrication: encapsulation of perovskites by gas-phase alumina deposition. *The Journal of Physical Chemistry Letters*, 2021, 12(9): 2348–2357
 118. Takada Y, Tsuji T, Okamoto N, Saito T, Kondo K, Yoshimura T, Fujimura N, Higuchi K, Kitajima A, Oshima A. Aluminum-doped zinc oxide electrode for robust (Pb,La)(Zr,Ti)O₃ capacitors: effect of oxide insulator encapsulation and oxide buffer layer. *Journal of Materials Science: Materials in Electronics*, 2014, 25(5): 2155–2161
 119. Fuentes-Fernandez E M A, Salomon-Preciado A M, Gnade B E, Quevedo-Lopez M A, Shah P, Alshareef H N. Fabrication of relaxer-based piezoelectric energy harvesters using a sacrificial poly-Si seeding layer. *Journal of Electronic Materials*, 2014, 43(11): 3898–3904
 120. Steinmann V, Moro L. Encapsulation requirements to enable stable organic ultra-thin and stretchable devices. *Journal of Materials Research*, 2018, 33(13): 1925–1936

121. Tu S H, Chen M, Wu L M. Dual-encapsulation for highly stable all-inorganic perovskite quantum dots for long-term storage and reuse in white light-emitting diodes. *Chemical Engineering Journal*, 2021, 412: 128688
122. Rathore S, Singh A. Bending fatigue damage reduction in indium tin oxide (ITO) by polyimide and ethylene vinyl acetate encapsulation for flexible solar cells. *Engineering Research Express*, 2020, 2(1): 015022
123. Luo Z D, Zhang C P, Yang L, Zhang J B. Ambient spray coating of organic-inorganic composite thin films for perovskite solar cell encapsulation. *ChemSusChem*, 2022, 15(3): e202102008
124. Jiang Y, Qiu L B, Juarez-Perez E J, Ono L K, Hu Z H, Liu Z H, Wu Z F, Meng L Q, Wang Q J, Qi Y B. Reduction of lead leakage from damaged lead halide perovskite solar modules using self-healing polymer-based encapsulation. *Nature Energy*, 2019, 4(7): 585–593
125. Dong Q S, Chen M, Liu Y H, Eickemeyer F T, Zhao W D, Dai Z H, Yin Y F, Jiang C, Feng J S, Jin S Y, Liu S Z, Zakeeruddin S M, Grätzel M, Padture N P, Shi Y T. Flexible perovskite solar cells with simultaneously improved efficiency, operational stability, and mechanical reliability. *Joule*, 2021, 5(6): 1587–1601
126. Shi Y R, Chen C H, Lou Y H, Wang Z K. Strategies of perovskite mechanical stability for flexible photovoltaics. *Materials Chemistry Frontiers*, 2021, 5(20): 7467–7478
127. Ye J J, Liu G Z, Jiang L, Zheng H Y, Zhu L Z, Zhang X H, Wang H X, Pan X, Dai S Y. Crack-free perovskite layers for high performance and reproducible devices via improved control of ambient conditions during fabrication. *Applied Surface Science*, 2017, 407: 427–433
128. Wang H P, Li S Y, Liu X Y, Shi Z F, Fang X S, He J H. Low-dimensional metal halide perovskite photodetectors. *Advanced Materials*, 2021, 33(7): 2003309
129. Jeon Y P, Woo S J, Kim T W. Transparent and flexible photodetectors based on $\text{CH}_3\text{NH}_3\text{PbI}_3$ perovskite nanoparticles. *Applied Surface Science*, 2018, 434: 375–381
130. Asuo I M, Fourmont P, Ka I, Gedamu D, Bouzidi S, Pignolet A, Nechache R, Cloutier S G. Highly efficient and ultrasensitive large-area flexible photodetector based on perovskite nanowires. *Small*, 2019, 15(1): 1804150
131. Wu D J, Xu Y C, Zhou H, Feng X, Zhang J Q, Pan X Y, Gao Z, Wang R, Ma G K, Tao L, Wang H B, Duan J X, Wan H Z, Zhang J, Shen L P, Wang H, Zhai T Y. Ultrasensitive, flexible perovskite nanowire photodetectors with long-term stability exceeding 5000 h. *InfoMat*, 2022, 4(9): e12320
132. Zheng W, Lin R C, Zhang Z J, Liao Q X, Liu J J, Huang F. An ultrafast-temporally-responsive flexible photodetector with high sensitivity based on high-crystallinity organic-inorganic perovskite nanoflake. *Nanoscale*, 2017, 9(34): 12718–12726
133. Shen K, Xu H, Li X, Guo J, Sathasivam S, Wang M Q, Ren A B, Choy K L, Parkin I P, Guo Z X, Wu J. Flexible and self-powered photodetector arrays based on all-inorganic CsPbBr_3 quantum dots. *Advanced Materials*, 2020, 32(22): 2000004
134. Perumal Veeramalai C, Yang S Y, Wei J Q, Sulaman M, Zhi R N, Saleem M I, Tang Y, Jiang Y R, Zou B S. Porous single-wall carbon nanotube templates decorated with all-inorganic perovskite nanocrystals for ultraflexible photodetectors. *ACS Applied Nano Materials*, 2020, 3(1): 459–467
135. Zheng J L, Luo C Z, Shabbir B, Wang C J, Mao W X, Zhang Y P, Huang Y M, Dong Y M, Jasieniak J J, Pan C X, Bao Q L. Flexible photodetectors based on reticulated SWNT/perovskite quantum dot heterostructures with ultrahigh durability. *Nanoscale*, 2019, 11(16): 8020–8026
136. Wu D J, Zhou H, Song Z H, Zheng M, Liu R H, Pan X Y, Wan H Z, Zhang J, Wang H, Li X M, Zeng H B. Welding perovskite nanowires for stable, sensitive, flexible photodetectors. *ACS Nano*, 2020, 14(3): 2777–2787
137. Deng H, Yang X K, Dong D D, Li B, Yang D, Yuan S J, Qiao K K, Cheng Y B, Tang J, Song H S. Flexible and semitransparent organolead triiodide perovskite network photodetector arrays with high stability. *Nano Letters*, 2015, 15(12): 7963–7969
138. Oh H, Jin Kim H, Kim S, Kim J A, Kang G M, Park M. Highly flexible and stable perovskite/microbead hybrid photodetectors with improved interfacial light trapping. *Applied Surface Science*, 2021, 544: 148850
139. Saraf R, Fan H, Maheshwari V. Porous perovskite films integrated with Au–Pt nanowire-based electrodes for highly flexible large-area photodetectors. *npj Flexible Electronics*, 2020, 4(1): 30
140. Zhan Y, Cheng Q F, Peng J S, Zhao Y, Vogelbacher F, Lai X T, Wang F Y, Song Y L, Li M Z. Nacre inspired robust self-encapsulating flexible perovskite photodetector. *Nano Energy*, 2022, 98: 107254
141. Meng X C, Cai Z R, Zhang Y Y, Hu X T, Xing Z, Huang Z Q, Huang Z D, Cui Y J, Hu T, Su M, Liao X F, Zhang L, Wang F Y, Song Y L, Chen Y W. Bio-inspired vertebral design for scalable and flexible perovskite solar cells. *Nature Communications*, 2020, 11(1): 3016
142. Wen X X, Lu Z H, Valdman L, Wang G C, Washington M, Lu T M. High-crystallinity epitaxial Sb_2Se_3 thin films on mica for flexible near-infrared photodetectors. *ACS Applied Materials & Interfaces*, 2020, 12(31): 35222–35231
143. Schneider D S, Grundmann A, Bablich A, Passi V, Kataria S, Kalisch H, Heuken M, Vescan A, Neumaier D, Lemme M C. Highly responsive flexible photodetectors based on MOVPE grown uniform few-layer MoS_2 . *ACS Photonics*, 2020, 7(6): 1388–1395
144. Li P, Hao Q Y, Liu J D, Qi D Y, Gan H B, Zhu J Q, Liu F, Zheng Z J, Zhang W J. Flexible photodetectors based on all-solution-processed Cu electrodes and in-se nanoflakes with high stabilities. *Advanced Functional Materials*, 2022, 32(10): 2108261
145. Yu G, Liu Z, Xie X M, Ouyang X, Shen G Z. Flexible photodetectors with single-crystalline GaTe nanowires. *Journal of Materials Chemistry C*, 2014, 2(30): 6104–6110
146. An J N, Le T S D, Lim C H J, Tran V T, Zhan Z Y, Gao Y, Zheng L X, Sun G Z, Kim Y J. Single-step selective laser writing of flexible photodetectors for wearable optoelectronics. *Advanced Science*, 2018, 5(8): 1800496
147. Wang Y H, Yang Z B, Li H R, Li S, Zhi Y S, Yan Z Y, Huang X, Wei X H, Tang W H, Wu Z P. Ultrasensitive flexible solar-blind photodetectors based on graphene/amorphous Ga_2O_3 van der Waals heterojunctions. *ACS Applied Materials & Interfaces*, 2020, 12(42): 47714–47720

148. Tong S C, Sun J, Wang C H, Huang Y L, Zhang C J, Shen J Q, Xie H P, Niu D M, Xiao S, Yuan Y B, He J, Yang J L, Gao Y L. High-performance broadband perovskite photodetectors based on $\text{CH}_3\text{NH}_3\text{PbI}_3/\text{C8BTBT}$ heterojunction. *Advanced Electronic Materials*, 2017, 3(7): 1700058
149. Hu X, Zhang X D, Liang L, Bao J, Li S, Yang W L, Xie Y. High-performance flexible broadband photodetector based on organolead halide perovskite. *Advanced Functional Materials*, 2014, 24(46): 7373–7380
150. Li C L, Lu J R, Zhao Y, Sun L Y, Wang G X, Ma Y, Zhang S M, Zhou J R, Shen L, Huang W. Highly sensitive, fast response perovskite photodetectors demonstrated in weak light detection circuit and visible light communication system. *Small*, 2019, 15(44): 1903599
151. Leung S F, Ho K T, Kung P K, Hsiao V K S, Alshareef H N, Wang Z L, He J H. A self-powered and flexible organometallic halide perovskite photodetector with very high detectivity. *Advanced Materials*, 2018, 30(8): 1704611
152. Saidaminov M I, Adinolfi V, Comin R, Abdelhady A L, Peng W, Dursun I, Yuan M J, Hoogland S, Sargent E H, Bakr O M. Planar-integrated single-crystalline perovskite photodetectors. *Nature Communications*, 2015, 6(1): 8724
153. Jung H R, Cho Y, Jo W. UV and visible photodetectors of MAPbBr_3 and MAPbCl_3 perovskite single crystals via single photocarrier transport design. *Advanced Optical Materials*, 2022, 10(7): 2102175
154. Chen Z L, Li C L, Zhumekenov A A, Zheng X P, Yang C, Yang H Z, He Y, Turedi B, Mohammed O F, Shen L, Bakr O M. Solution-processed visible-blind ultraviolet photodetectors with nanosecond response time and high detectivity. *Advanced Optical Materials*, 2019, 7(19): 1900506
155. Zhou Y, Qiu X, Wan Z A, Long Z H, Poddar S, Zhang Q P, Ding Y C, Chan C L J, Zhang D Q, Zhou K M, Lin Y J, Fan Z Y. Halide-exchanged perovskite photodetectors for wearable visible-blind ultraviolet monitoring. *Nano Energy*, 2022, 100: 107516
156. Li Y, Shi Z F, Li S, Lei L Z, Ji H F, Wu D, Xu T T, Tian Y T, Li X J. High-performance perovskite photodetectors based on solution-processed all-inorganic CsPbBr_3 thin films. *Journal of Materials Chemistry C*, 2017, 5(33): 8355–8360
157. Cen G B, Liu Y J, Zhao C X, Wang G, Fu Y, Yan G H, Yuan Y, Su C H, Zhao Z J, Mai W J. Atomic-layer deposition-assisted double-side interfacial engineering for high-performance flexible and stable CsPbBr_3 perovskite photodetectors toward visible light communication applications. *Small*, 2019, 15(36): 1902135
158. Zhu Z H, Deng W, Li W, Chun F J, Luo C, Xie M L, Pu B, Lin N, Gao B, Yang W Q. Antisolvent-induced fastly grown all-inorganic perovskite CsPbCl_3 microcrystal films for high-sensitive UV photodetectors. *Advanced Materials Interfaces*, 2021, 8(6): 2001812
159. Gong M G, Sakidja R, Goul R, Ewing D, Casper M, Stramel A, Elliot A, Wu J Z. High-performance all-inorganic CsPbCl_3 perovskite nanocrystal photodetectors with superior stability. *ACS Nano*, 2019, 13(2): 1772–1783
160. Hou Z L, Liu X Y, Wen G J, Jiang S L. Enhancing the photoelectric performance of the self-powered all vapor-deposited CsPbCl_3 ultraviolet photodetectors by a novel cadmium-doping strategy and heterojunction engineering. *Solar Energy Materials and Solar Cells*, 2023, 251: 112175
161. Yang L, Tsai W L, Li C S, Hsu B W, Chen C Y, Wu C I, Lin H W. High-quality conformal homogeneous all-vacuum deposited CsPbCl_3 thin films and their UV photodiode applications. *ACS Applied Materials & Interfaces*, 2019, 11(50): 47054–47062
162. Lei L Z, Shi Z F, Li Y, Ma Z Z, Zhang F, Xu T T, Tian Y T, Wu D, Li X J, Du G T. High-efficiency and air-stable photodetectors based on lead-free double perovskite $\text{Cs}_2\text{AgBiBr}_6$ thin films. *Journal of Materials Chemistry C*, 2018, 6(30): 7982–7988
163. Shuang Z H, Zhou H, Wu D J, Zhang X H, Xiao B A, Ma G K, Zhang J, Wang H. Low-temperature process for self-powered lead-free $\text{Cs}_2\text{AgBiBr}_6$ perovskite photodetector with high detectivity. *Chemical Engineering Journal*, 2022, 433: 134544
164. Yan G H, Jiang B Q, Xiao Y, Zhao C X, Yuan Y, Liang Z C. Alkali metal ions induced high-quality all-inorganic $\text{Cs}_2\text{AgBiBr}_6$ perovskite films for flexible self-powered photodetectors. *Applied Surface Science*, 2022, 579: 152198
165. Syazwani C J N, Wahab N H A, Sunar N, Ariffin S H S, Wong K Y, Aun Y. Indoor positioning system: a review. *International Journal of Advanced Computer Science and Applications*, 2022, 13(6): 477–490
166. Salih K O M, Rashid T A, Radovanovic D, Bacanin N. A comprehensive survey on the internet of things with the industrial marketplace. *Sensors*, 2022, 22(3): 730
167. Mohsin M J, Mudas I A. Design an outdoor light fidelity (Li-Fi) system based on all-optical OFDM architecture. *International Journal of Intelligent Engineering and Systems*, 2022, 15(3): 193–204
168. Cao Y, Zheng Y F, Wang X, Liu Y B, Liu Y. Research and prospect on key technologies of indoor positioning based on visible light communication. *Journal of Physics: Conference Series*, 2022, 2160(1): 012074
169. Liu R H, Zhang J Q, Zhou H, Song Z H, Song Z N, Grice C R, Wu D J, Shen L P, Wang H. Solution-processed high-quality cesium lead bromine perovskite photodetectors with high detectivity for application in visible light communication. *Advanced Optical Materials*, 2020, 8(8): 1901735
170. Huang B, Liu J X, Han Z Y, Gu Y, Yu D J, Xu X B, Zou Y S. High-performance perovskite dual-band photodetectors for potential applications in visible light communication. *ACS Applied Materials & Interfaces*, 2020, 12(43): 48765–48772
171. Mohsan S A H, Mazinani A, Sadiq H B, Amjad H. A survey of optical wireless technologies: practical considerations, impairments, security issues and future research directions. *Optical and Quantum Electronics*, 2022, 54(3): 187
172. Schmid S, Ziegler J, Corbellini G, Gross T R, Mangold S. Using consumer led light bulbs for low-cost visible light communication systems. In: *Proceedings of the 1st ACM MobiCon Workshop on Visible Light Communication Systems*. Hawaii: Association for Computing Machinery, 2014, 9–14
173. Dutta A K. Imaging beyond human vision. In: *Proceedings of the 8th International Conference on Electrical and Computer Engineering*. Dhaka: IEEE, 2014, 224–229
174. Nikzad S. High-performance silicon imagers and their applications in astrophysics, medicine and other fields. In: *Nikzad*

- S, ed. *High Performance Silicon Imaging*. Woodhead Publishing, 2014, 411–438
175. Lee S M, Biswas R, Li W G, Kang D, Chan L, Yoon J. Printable nanostructured silicon solar cells for high-performance, large-area flexible photovoltaics. *ACS Nano*, 2014, 8(10): 10507–10516
176. Lee S Y, Kim S H, Hwang H, Sim J Y, Yang S M. Controlled pixelation of inverse opaline structures towards reflection-mode displays. *Advanced Materials*, 2014, 26(15): 2391–2397
177. Sakanoue T, Mizukami M, Oku S, Yoshimura Y, Abiko M, Tokito S. Fluorosurfactant-assisted photolithography for patterning of perfluoropolymers and solution-processed organic semiconductors for printed displays. *Applied Physics Express*, 2014, 7(10): 101602
178. Xia K L, Wu W Q, Zhu M J, Shen X Y, Yin Z, Wang H M, Li S, Zhang M C, Wang H M, Lu H J, Pan A L, Pan C F, Zhang Y Y. CVD growth of perovskite/graphene films for high-performance flexible image sensor. *Science Bulletin*, 2020, 65(5): 343–349
179. van Breemen A J J M, Olleary R, Shanmugam S, Peeters B, Peters L C J M, van de Ketterij R L, Katsouras I, Akkerman H B, Frijters C H, Di Giacomo F, Veenstra S, Andriessen R, Janssen R A J, Meulenkaamp E A, Gelinck G H. A thin and flexible scanner for fingerprints and documents based on metal halide perovskites. *Nature Electronics*, 2021, 4(11): 818–826
180. Jang J, Park Y G, Cha E, Ji S, Hwang H, Kim G G, Jin J, Park J U. 3D heterogeneous device arrays for multiplexed sensing platforms using transfer of perovskites. *Advanced Materials*, 2021, 33(30): 2101093
181. Gu L L, Poddar S, Lin Y J, Long Z H, Zhang D Q, Zhang Q P, Shu L, Qiu X, Kam M, Javey A, Fan Z Y. A biomimetic eye with a hemispherical perovskite nanowire array retina. *Nature*, 2020, 581(7808): 278–282
182. Li H, Zhang Y, Zhou M, Ding H Y, Zhao L, Jiang T M, Yang H Y, Zhao F, Chen W Q, Teng Z W, Qiu J B, Yu X, Yang Y M, Xu X H. A solar-blind perovskite scintillator realizing portable X-ray imaging. *ACS Energy Letters*, 2022, 7(9): 2876–2883
183. Alfonso C, Garcia-Gonzalez M A, Parrado E, Gil-Rojas J, Ramos-Castro J, Capdevila L. Agreement between two photoplethysmography-based wearable devices for monitoring heart rate during different physical activity situations: a new analysis methodology. *Scientific Reports*, 2022, 12(1): 15448
184. Li C C, Chen H M, Zhang S C, Yang W, Gao M, Huang P Y, Wu M Q, Sun Z Y, Wang J, Wei X. Wearable and biocompatible blood oxygen sensor based on heterogeneously integrated lasers on a laser-induced graphene electrode. *ACS Applied Electronic Materials*, 2022, 4(4): 1583–1591